POSIVA 2007-01

Drill Hole Logging Device TERO76 for Determination of Rock Thermal Properties

Posiva Oy

February 2007

POSIVA OY
FIN-27160 OLKILUOTO, FINLAND
Phone (02) 8372 31 (nat.), (+358-2-) 8372 31 (int.)
Fax (02) 8372 3709 (nat.), (+358-2-) 8372 3709 (int.)

POSIVA 2007-01

Drill Hole Logging Device TERO76 for Determination of Rock Thermal Properties

Ilmo Kukkonen
Ilkka Suppala
Arto Korpisalo
Geological Survey of Finland

Teemu Koskinen
Stips Oy

February 2007

POSIVA OY
FI-27160 OLKILUOTO, FINLAND
Phone (02) 8372 31 (nat.), (+358-2-) 8372 31 (int.)
Fax (02) 8372 3709 (nat.), (+358-2-) 8372 3709 (int.)

ISBN 978-951-652-149-0
ISSN 1239-3096

Posiva-raportti – Posiva Report

Posiva Oy
FI-27160 OLKILUOTO, FINLAND
Puh. 02-8372 (31) – Int. Tel. +358 2 8372 (31)

Raportin tunnus – Report code
POSIVA 2007-01

Julkaisuaika – Date
February 2007

Tekijä(t) – Author(s)

Ilmo Kukkonen, Geological Survey of Finland
Ilkka Suppala, Geological Survey of Finland
Arto Korpisalo, Geological Survey of Finland
Teemu Koskinen, Stips Oy

Toimeksiantaja(t) – Commissioned by

Posiva Oy

Nimeke – Title

DRILL HOLE LOGGING DEVICE TERO76 FOR DETERMINATION OF ROCK THERMAL PROPERTIES

Tiivistelmä – Abstract

A new version of the TERO thermal drill hole device for determining thermal properties of rocks in situ in slim drill holes is presented. We have constructed a new tool ("TERO76") for 76 mm drill holes. Similarly to the drill hole tool for 56 mm holes ("TERO56") the new device is based on conduction of heat from a cylindrical heat source placed in a drill hole. The down-hole probe is built of a hollow aluminium cylinder, which is 1640 mm long and whose outer diameter is 70 mm. A foil-like heating resistor is placed on the inner surface of the hollow cylinder. The length of the heating section of the cylinder is 1.5 m. The applied maximum heating power is 49 W. Heating power is monitored during measurements. 28 NTC thermistors are placed in four lines along the inner surface of the aluminium cylinder. Convection in the hole is prevented with soft silicon rubber packers. The instrument is pressure-proof up to 700 m in water-filled holes. The major differences between the TERO56 and TERO76 probes, in addition to dimensions, are related to the increased maximum heating power, improved measurement of heating power and the reduced level of undesired heat generation of the electronics in the TERO76 probe.

Test measurements of the TERO76 tool were carried out in Olkiluoto in drill hole OL-KR14 in March 2006. The main rock types of the drill hole are mica gneiss, tonalite and granite. Measurements were done at six depth levels between 394 and 465 m using a heating time of 6 h followed by a cooling time of 12 h. Measurements at five depth levels were disturbed by fluid flow effects during measurements (leakage of packers), but the effects were small, and did not prevent inversion for rock thermal properties.

The thermal property estimation is based on fitting measured temperature data with forward modelling of conductive heat transfer from a cylinder source with finite length and conductivity (2-dimensional cylinder symmetric finite element model). The inverted values of thermal properties are in general agreement with previous data on the thermal properties of mica gneiss and granitoid rocks in Olkiluoto. The inverted thermal conductivities range from 2.95 to 3.78 W m^{-1} K^{-1}, and diffusivity from 1.51 to 2.30 $\cdot 10^{-6}$ m^2 s^{-1}.

Avainsanat - Keywords

thermal conductivity, specific heat capacity, thermal diffusivity, nuclear waste disposal, Olkiluoto, mica gneiss, tonalite, granite, in situ measurement

ISBN	ISSN
ISBN 978-951-652-149-0	ISSN 1239-3096
Sivumäärä – Number of pages: 38	Kieli – Language: English

Posiva-raportti – Posiva Report

Posiva Oy
FI-27160 OLKILUOTO, FINLAND
Puh. 02-8372 (31) – Int. Tel. +358 2 8372 (31)

Raportin tunnus – Report code
POSIVA 2007-01

Julkaisuaika – Date
Helmikuu 2007

Tekijä(t) – Author(s)

Ilmo Kukkonen, GTK
Ilkka Suppala, GTK
Arto Korpisalo, GTK
Teemu Koskinen, Stips Oy

Toimeksiantaja(t) – Commissioned by

Posiva Oy

Nimeke – Title

TERO76 - REIKÄLUOTAUSLAITTEISTO KIVIEN TERMISTEN OMINAISUUKSIEN MÄÄRITTÄMISEEN

Tiivistelmä – Abstract

Tässä työssä esitellään uusi versio kallion termisten ominaisuuksien reikämittauksiin tarkoitetusta ”TERO-laitteistosta”. Halkaisijaltaan 76 mm reikiä varten on rakennettu uusi reikäanturi. Kuten aikaisempi, 56 mm:n kairareikiin tarkoitettu TERO56-laitteisto, uusi TERO76-laitteisto perustuu sylinterimäisen lämpölähteen lämpötilavasteeseen, joka riippuu lämmitystehon lisäksi ympäröivän väliaineen lämmönjohtavuudesta ja diffusiviteetistä. Anturi on rakennettu alumiiniputkesta, jonka pituus on 1640 mm ja ulkohalkaisija 70 mm. Kalvomainen lämmitin, jonka pituus on 1500 mm, on asennettu putken sisäpinnalle. Lämmitysteho on maksimissaan 49 W. 28 kpl NTC-pintaliitostermistoreita on asennettu neljään jonoon pitkin alumiiniputken sisäpintaa. Lämmitystehoa seurataan jatkuvasti. Veden pystysuuntainen virtaus reiässä estetään pehmeiden silikonikumipakkereiden avulla. Laite on paineenkestävä 700 m syvyyteen saakka. Olennaiset erot TERO56- ja TERO76-laitteiden välillä (ulkoisten mittojen lisäksi) liittyvät TERO76-anturin korkeampaan maksimilämmitystehoon ja parannettuun tehon mittaukseen. Lisäksi mittauselektroniikan synnyttämää haitallista lämmöntuottoa on voitu pienentää.

Laitetta testattiin Olkiluodossa kairareikä OL-KR14:ssä maaliskuussa 2006. Tutkimusreiän pääkivilajit ovat kiillegneissi, tonaliitti ja graniitti. Mittauksia tehtiin kuudella eri syvyydellä välillä 394 - 465 m käyttäen 6 h lämmitysaikaa ja 12 tunnin jäähtymisaikaa. Viidellä mittaussyvyydellä todettiin pakkerivuotojen aiheuttamia häiriöitä, mutta ne eivät olleet niin suuria, ettei tuloksista voitaisi laskea kallion termisten ominaisuuksien arvoja.

Anturin lämpötilavaste on laskettu elementtimenetelmällä käyttäen äärellisen pitkän sylinterisymmetrisen lämpölähteen lämmönjohtumismallia. Kallion termiset ominaisuudet laskettiin inversiolla käyttäen pienimmän neliösumman menetelmään perustuvaa optimointimenetelmää. Tulokset ovat yhteensopivia aikaisemmin Olkiluodon kiillegneissistä, tonaliitista ja graniitista tehtyjen laboratoriomittausten kanssa. Inversiolla ratkaistut lämmönjohtavuudet ovat välillä 2.95 - 3.78 W m^{-1} K^{-1}, ja diffusiviteetit välillä 1.51 - 2.30 · 10^{-6} m^2 s^{-1} .

Avainsanat - Keywords

lämmönjohtavuus, ominaislämpökapasiteetti, terminen diffusiviteetti, ydinjätteiden loppusijoitus, kiillegneissi, tonaliitti, graniitti, Olkiluoto

ISBN
ISBN 978-951-652-149-0

ISSN
ISSN 1239-3096

Sivumäärä – Number of pages
38

Kieli – Language
Englanti

TABLE OF CONTENTS

PREFACE

The study has been carried out at the Geological Survey of Finland (GTK) on contract for Posiva Oy. On behalf of the orderer, the supervising of the work was done by Maiju Paunonen, Aimo Hautojärvi (Posiva Oy) and Erik Johansson (Saanio & Riekkola Oy). The geophysical design, equipment, construction, measurements, software development, interpretation and reporting were done by Ilmo Kukkonen, Ilkka Suppala, Arto Korpisalo (GTK) and Teemu Koskinen (Stips Oy).

1 INTRODUCTION

Thermal parameters of rocks are necessary data in planning final repository for spent nuclear fuel in deep bedrock. The thermal properties of rocks can be determined with laboratory measurements of core samples, theoretical calculations from mineral composition and data on properties of the constituent minerals, and with in situ measurements in drill holes. Laboratory measurements and theoretical calculations on thermal properties of rocks at Olkiluoto and other disposal candidate sites in Finland have been presented previously by Kjørholt (1992), Kukkonen and Lindberg (1995, 1998) and Kukkonen (2000). A comparison between different laboratory measurements applied in site studies in Finland and Sweden has been given by Sundberg et al. (2003).

In situ measurements have been under development in Posiva since 1999. Kukkonen and Suppala (1999) summarized the literature data on various in situ techniques and carried out theoretical simulations of in situ measurements. A prototype and test version of an in situ drill hole tool, based on temperature response of a heated cylindrical probe, was built and applied in 1999 by Kukkonen et al. (2000 and 2001). Thermal modelling was elaborated from simple 1-dimensional infinite line source and cylindrical sources into 2-dimensional finite element models including the internal structure of the probe, and the contact resistance layer between the in situ probe and drill hole wall as well as finitely long cylinder models (3D models). Based on this experience, the first version of production logging tool for 56 mm drill holes was designed and constructed by Suppala et al. (2004) and Kukkonen et al. (2005). The logging device is called with the acronym “TERO56” (earlier only “TERO”).

The basic properties of the TERO56 device and measurements carried out in a deep drill hole (OL-KR2) in Olkiluoto were reported by Kukkonen et al. (2005). The instrument was used for measurements in Oskarshamn, Sweden, in both 56 mm and 76 mm diameter drill holes (Kukkonen et al. 2006).

Due to the characteristics of the physical problem of estimating thermal properties of rocks in water-filled drill holes, it is necessary to minimize the thickness of the water layer between the probe and the drill hole wall. Measurement of holes with diameter larger than 56 mm with the TERO56 probe has proven difficult because of convective heat transfer by the drill hole fluid during measurements (Kukkonen et al. 2006). Therefore, it was decided to construct a new probe for 76 mm drill holes, which has the typical hole diameter applied for instance in the Olkiluoto repository site studies. We report here the construction, properties and results of test measurements with the new TERO76 probe.

2 DRILL HOLE LOGGING DEVICE TERO76

The TERO76 probe is used with the same winch and cable as the TERO56 probe (Suppala et al. 2004). The complete logging device comprises the drill hole tool, logging cable and winch together with the computer and current source located at the surface. The winch and steel armoured cable were purchased from the German company LogIn GmbH, and they represent standard geophysical logging instrumentation of the day. The cable is 700 m long steel armoured 4-conductor logging cable. The motorized winch is controlled from a separate control panel. In principle the winch system has an option of automated operation, but it is not included at the present TERO76 device.

A computer collects the depth data from the winch and with the aid of the control unit measured resistances from temperature sensors, heating current and voltage as well as the resistances of the single point resistance sensor.

The main components of the TERO76 device are shown in Figure 1. The system at the GTK test hole in Espoo is depicted in Figure 2.

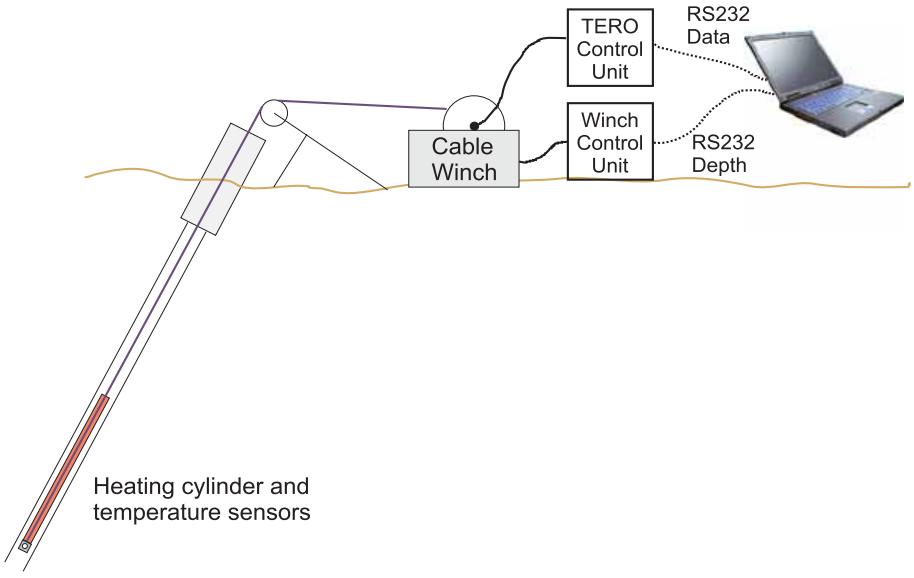

Figure 1. *The components of the TERO76 logging device.*

Figure 2. *TERO logging device at the GTK test hole, Espoo.*

The basic properties of the TERO76 device are as follows:

- Determination of thermal conductivity and diffusivity in situ in 76 mm water-filled drill holes
- The measurement principle: Thermal response of a heated cylinder
- Length of cable is 700 m, motorized winch
- The outer diameter of probe is 70 mm
- Length of the heated part of the probe is 1.5 m
- Heating power is 49 W at maximum
- Monitoring of heating power is carried out from the probe and cable at surface
- Heating takes place with heating foils installed at the inner surface of the probe tube
- Flow of water along the measurement section is prevented with soft packers made of silicon rubber
- Number of NTC temperature sensors is 28, located around the probe along four axial lines, resolution 0.5 mK, range 4-30 ºC
- A galvanic single point sensor is included in the tool for precise determination of logging depth with the aid of fracture anomalies
- Determination of tool orientation is done with the magnetic field (3-component flux gate sensors) and inclination (acceleration) sensors.

3 MEASUREMENT PRINCIPLE AND MECHANICAL CONSTRUCTION OF THE TERO76 LOGGING DEVICE

3.1 Principle of measuring rock thermal properties in a drill hole

The measurement principle of the TERO76 device is the same as that of the TERO56 device (Suppala et al. 2004, Kukkonen et al. 2005). Let us assume a situation where the in situ probe is initially in a drill hole under thermal stationary conditions. When the probe is heated, its temperature as a function of time depends on the applied heating power, heat losses into rock, and the thickness of the water layer between the probe and drill hole wall. Temperatures are also dependent on the internal structure of the probe and its material properties. In the present study the probe properties are taken into account as solid parameters of the time-dependent heat conduction model. The remaining parameters, which need to be estimated are thermal properties of the surrounding medium. In a drill hole, the probe is (mostly) immersed in water, and the thickness of the water layer varies with varying hole calliper. In the interpretation the water layer, acting as a heat capacitor and resistance, must be taken into account.

The linear equation of conduction of heat giving the temperature T (**r**,t), dependent on the location **r** (location vector in a Cartesian coordinate system) and on time t, is (Carslaw & Jaeger 1959, Jarny et al. 1991):

$$\rho\, c(\mathbf{r}) \frac{\partial T(\mathbf{r},t)}{\partial t} = \nabla \cdot (\boldsymbol{\lambda}(\mathbf{r})\, \nabla T(\mathbf{r},t)) + g(\mathbf{r},t) \tag{3.1}$$

In equation 3.1 $\boldsymbol{\lambda}$ is thermal conductivity, which is a tensor variable (W m^{-1} K^{-1}), ρc is heat capacity (density · specific heat capacity) (J m^{-3} K^{-1}) and g is heating power (Wm^{-3}). Thermal diffusivity is the ratio of thermal conductivity and heat capacity $s = \lambda/\rho c$. Dividing both sides of equation 3.1 by ρc shows that the problem can be also described in terms of thermal diffusivity and heat capacity.

Temperature increase of an infinitely long cylinder having an infinite conductivity and situated in a homogeneous space can be presented with an analytical solution (Carslaw & Jaeger 1959). Such a solution was used in the first examinations of the applications of the method as well as in the interpretations (Kukkonen & Suppala 1999, Kukkonen et al. 2000). The analytical solution, however, is not sufficient for describing the modelling of a cylinder with finite length and conductivity, nor is it able to handle the contact resistance effects between the probe and drill hole wall. Therefore we have applied here numerical finite element techniques with the COMSOL Multiphysics® software. Our models are a (i) cylindrically symmetric, infinitely long probe (1-D element mesh), (ii) infinitely long probe (2-D element mesh) and (iii) a finite cylindrically symmetric probe (2-D element mesh).

The forward modelling of the problem is carried out with the numerical solution of equation 3.1. The unknown variables, thermal conductivity or diffusivity of rock and the thermal contact resistance or alternatively, the thickness of the water layer, are

estimated with the method of least squares using the measured and calculated probe temperatures. In previous reports (Kukkonen & Suppala 1999; Kukkonen et al. 2000, 2001, 2005) we have discussed the interpretation of the measurements in more detail.

According to sensitivity analysis of the theoretical simulations we can estimate that thermal conductivity can be determined at best with an error smaller than 2 % and diffusivity with less than 5 % error, given that the error in temperature measurements is smaller than ±0.03 K (Kukkonen et al. 2001). Determination of diffusivity depends strongly on contact resistance, i.e. the water layer thickness. In other words, this requires that the water layer thickness should be known for reliable determination of diffusivity.

3.2 Procedure of drill hole measurements

The drill hole measurements are done as follows. First, the probe is lowered to the measurement depth in the drill hole. The probe is allowed to equilibrate to the temperature over an hour, when it has reached a steady-state condition. The heating time can be chosen freely, and longer heating times involve larger volumes into the measurement around the drill hole. Theoretical considerations (Kukkonen & Suppala 1999) indicated that, for instance, 12-hour heating period influences the temperatures, that can be measured in practice, only to a distance of about 0.5 m from the drill hole wall. Therefore, the heating time can be pre-set to as long as 6-16 hours. Temperatures are registered during lowering of probe in the hole, thermal equilibration, as well as heating and cooling of the probe. Thus, the measurement of one depth station in the drill hole takes 12-24 hours. Only temperature changes during the heating and cooling periods are taken into account in the interpretation of the data. The most important temperature readings are obtained from the centre of the probe, where the approximation of an infinitely long cylinder is valid for longest times.

3.3 The mechanical construction of the TERO76 probe

The in situ probe is shown in Figure 3. The detailed construction drawings of the TERO76 probe are given in a separate Posiva Working Report (Kukkonen et al. 2007). Thermistors and heating resistors are placed on the inner surface of the aluminium pipe. The white plastic parts have been made of “Ertalyte” plastic, which is a semi-crystalline thermoplastic polyester based on polyethylene terephthalate (PET-P). The electronic circuit boards are located in the plastic parts of the upper and lower ends of the probe. The probe is pressure resistant up to 700 m of water depth. Flow along the drill hole is prevented with one or two pairs of soft packers made of silicon rubber produced by PRG-Tec Oy (Figure 4).

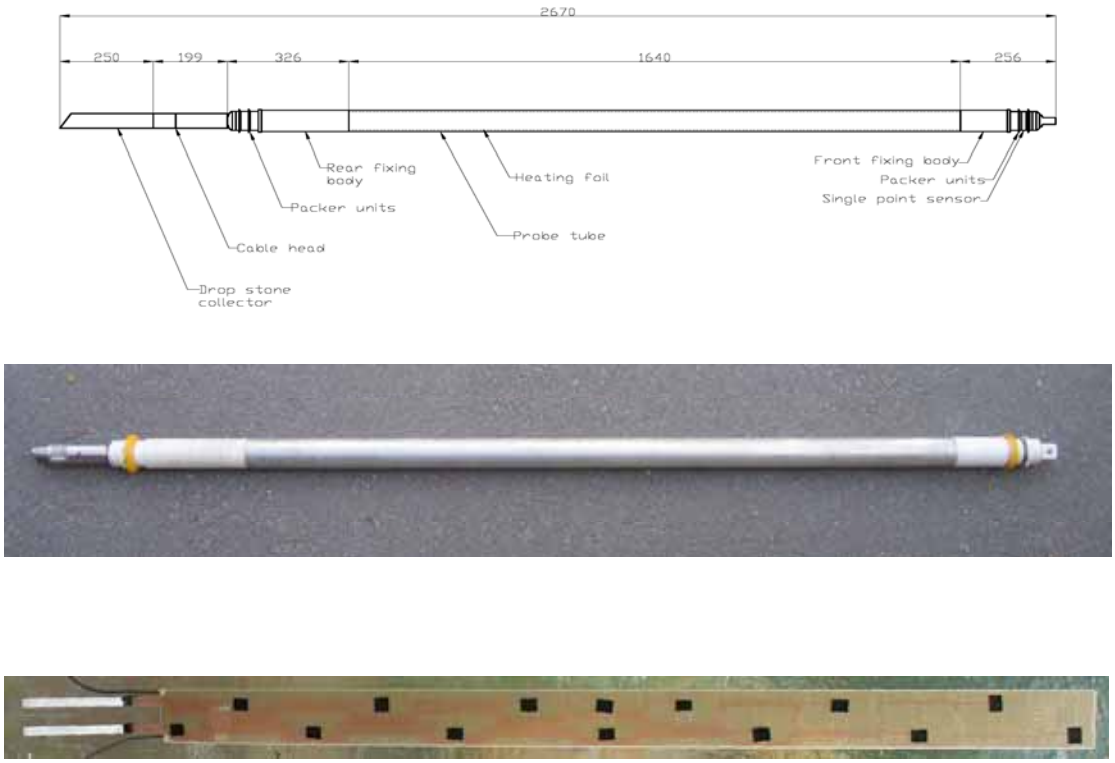

Figure 3. *Main parts and dimensions of the TERO76 in situ probe (above), the constructed probe (middle) and the heating and thermistor foil (bottom). The cable end is connected at the left end, and the additional weights are hanged at the right end of the probe.*

Figure 4. *The lower end of the TERO76 probe. The yellow part is the soft silicon rubber packer. The dark ring is the single-point galvanic sensor.*

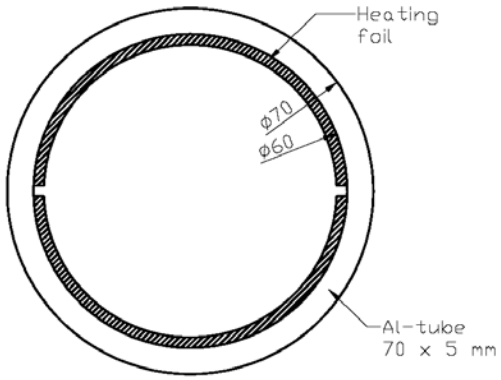

Figure 5. *Cross section of the probe showing the aluminium tube, heating and thermistor foil.*

The outer and inner diameters of the probe are 70 and 60 mm, respectively. Cross section of the probe is given in Figure 5. The thermal conductivity of the aluminium alloy (EN 6082-T6) is 172 W m^{-1} K^{-1} and heat capacity 2430870 (J m^{-3} K^{-1}) according to the producer of the pipe. Respectively, producer information provides a value 0.29 W m^{-1} K^{-1} for the thermal conductivity of the PET-P plastic.

In order to enhance positioning of the probe in depth, a galvanic single-point sensor is included in the probe (Figure 4). Extra weight is used at the lower end of the probe to aid the lowering of the probe into a drill hole. The weight is indispensable because the friction of the packers makes the lowering of the probe in the hole very slow. The extra weight material is lead in a brass tube with a mass of 40 kg. Detailed mechanical construction drawings are given in a Posiva Working Report (Kukkonen et al., 2007).

3.4 Heating foils and thermistors

The probe is heated with two heating foils (resistors) on the inner surface of the aluminium pipe. The foils provide homogeneous warming of the pipe. Thermistors and foils have been installed together. One of the heating foils with the thermistors is shown in Figures 3 and 6. The foils were purchased from Calesco Foils Ab. The foil producer was also responsible for installing the thermistors on the foils. We applied NTC thermistors by BCcomponents (type no. 232261513103). Their nominal resistance is 10000 Ω at 25 ºC. The total number of thermistors installed along the probe on four axial lines is 28. In addition, the electronics is monitored with four thermistors installed on the circuit boards.

The heating and thermistor foils are compressed against the inner surface of the aluminium pipe with a pressurized rubber tube. The length of the rubber tube is about equal to the length of the heating foils. The foils are not glued on the aluminium tube. Therefore, the heating foils and thermistors can be easily replaced and maintained.

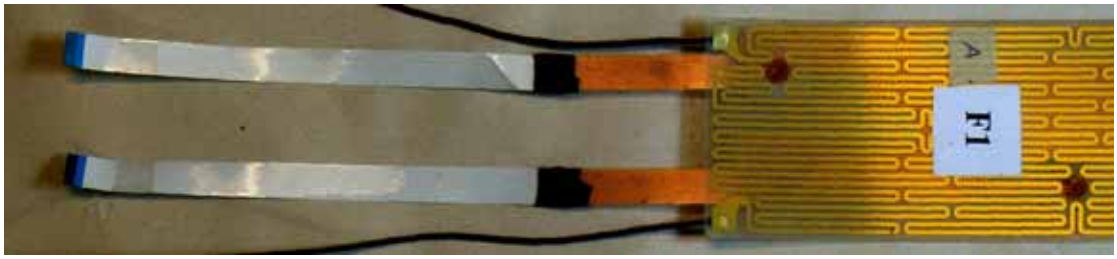

Figure 6. *A close-up of the upper ends of the heating and thermistor foils.*

The upper end of the foil is shown in Figure 6. The heating foil is actually a thin electric resistor made of brass and glued between resistive foils made of polyester plastic (thickness 0.075 mm). The temperature sensor foil has a set of copper conductors joining the thermistors with the circuit boards.

The resistance of the heating foils is about 100 Ω. In contrast to TERO56 electronics, the temperature dependence of the foil resistance plays no role in TERO76 heating power measurements, as the heating current and voltage are measured directly from the foil.

3.5 Electronics

Electronics responsible for measuring the temperatures and the single-point resistance has been installed in the upper end of the probe. In addition, the 2-component acceleration sensor and 3-component flux gate magnetometer have been installed at the lower end of the probe. Detailed circuit diagrams of the electronics are given by Kukkonen et al. 2007.

The recording and controlling PC and the control unit are at the surface containing the modem, voltage source for measurements as well as the current source for heating. The heating power is continuously monitored at the upper end of the cable. The resistance of the cable is 57 Ω.

3.6 Thermistor calibration

The thermistors were calibrated after installation on the heating foils. The both foils were placed inside a cylinder made of aluminium. The aluminium cylinder is 12 cm in diameter and 10 cm high. The cylinder was placed into a hole drilled into a cylindrical piece of concrete (diameter 25 cm, height 22 cm and mass of about 15 kg). Reference temperatures were taken with high accuracy laboratory thermometer (Hart Scientific, Model 1504, Serial No. A56472) capable of temperature measurements with an accuracy better than 1 mK. The reference thermometer is factory-calibrated. The sensing probe of the reference thermometer is a thermistor placed in a thin (3 mm)

Figure 7. *Arrangement of the temperature calibration of thermistor foils inside a piece of concrete. The foils are placed at the center of the concrete cylinder inside an aluminium pipe. At the center of the aluminium pipe there is a high accuracy thermistor probe (Hart Scientific, Model 1504). During measurements the structures were covered with insulating plastic. The complete installation was then placed in a thermally controlled box.*

needle probe. The reference thermometer was placed at the axis of the thermistor foil roll in the aluminium cylinder. The concrete piece was insulated with plastic and placed in a test box, the temperatures of which were kept stable with a thermostate. The temperature readings were followed with a computer (Figure 7).

The inside temperature of the test box could be observed in temperature readings taken outside the concrete cylinder as periodic temperature variations, but variations inside the cylinder were very slow. The resolution of the reference thermometer is 0.1 mK. The corresponding thermistors resistances were calculated as averages of 20-200 readings taken at 10 second intervals. Fifteen reference temperatures between 2-29 ºC were applied. The calibration curves of foils are shown in Figure 8.

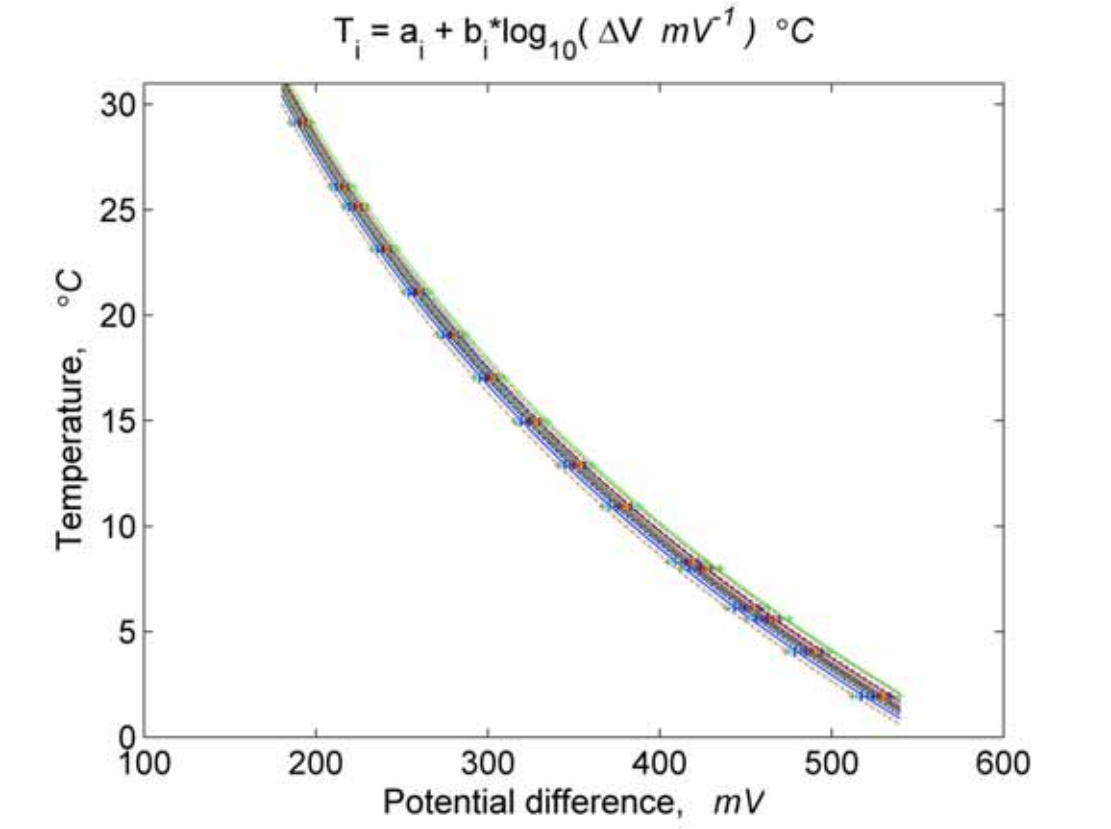

Figure 8. *Calibration curves of the thermistors obtained by measurements at fifteen reference temperature between 2-29 ºC.*

Thermistor temperatures are calculated from fitting a semi-logarithmic curve on measured voltage differences: $T_i()V) = a_i + b_i \log_{10}()U)$. Average fitted parameter values are a = 170.8 ± 0.9 and b = -62.02 ± 0.27. Generally, the fitted calibration curves were equally satisfactory. The median of the absolute fitting error was about 0.04 K in calibration of both foils.

For instance, the median values of deviations of all thermistor results recorded in 20-200 sequential readings taken at 10 s intervals is ±0.00026 K at the low temperature end and ±0.0007 K at the high temperature end, whereas the maximum deviations are smaller than ± 0.003 K. The error in fitting of the polynomial function is mainly due to hysteretic effects in warming and cooling of the concrete piece and slow equilibration of temperatures during the calibration process. Nevertheless, the calibration satisfies requirements of measuring temperatures with a maximum error smaller than 0.03 K yielding conductivity and diffusivity estimates better than ± 2 % and ± 5 %, respectively.

3.7 TERO Graphical interface

As a part of the system development a graphical interface system was designed and constructed for the TERO56 device (Kukkonen et al. 2005, Korpisalo 2005) (Figure 9). The same interface is applied with the TERO76 probe. TERO Graphical Interface (TGI) is a versatile analysis and interpretation toolbox, which is developed in MATLAB environment. The development work is done under Windows XP Operating System but XP is not a strict demand. To use the whole power of the TGI there should be at least 1 GB ROM memory (2 GB is recommended). In the case that

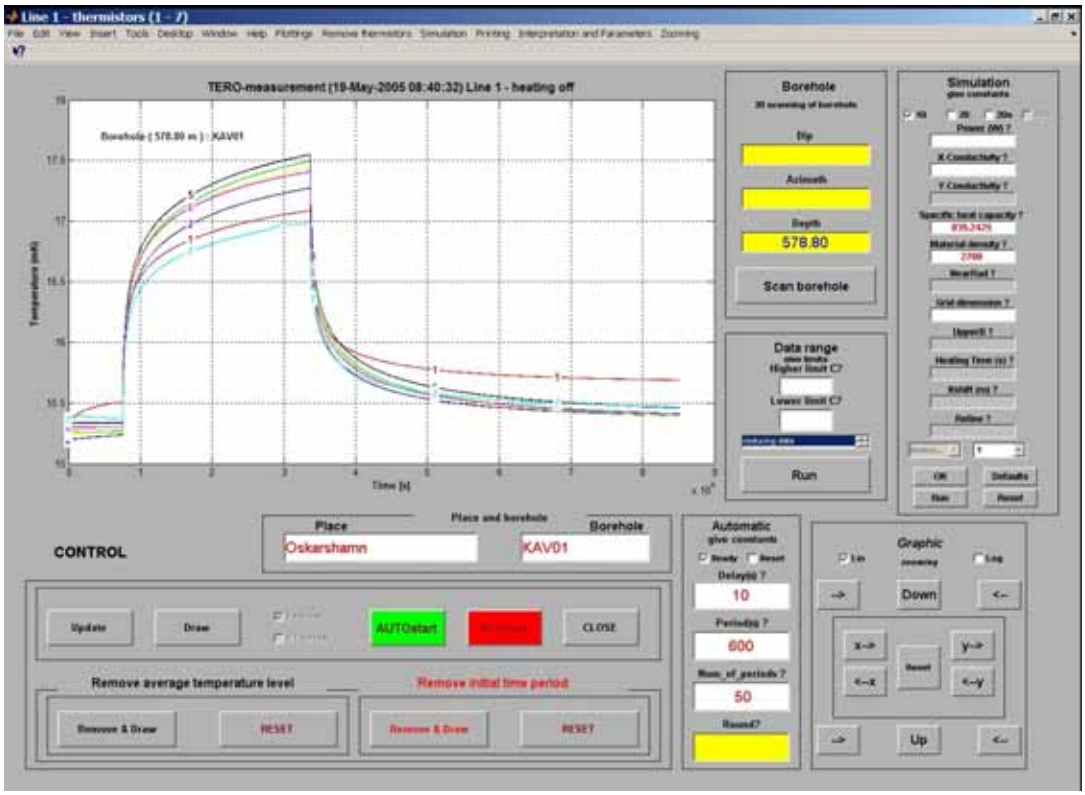

Figure 9. *View of the TERO graphical interface.*

MATLAB 6.5.1 or earlier versions are used, Java exception errors will be generated by the system. The system works best in the latest version of MATLAB (currently 7.0.1). In addition, the TGI system requires the latest version of FEMLAB (3.1).

Data analysis of temperature readings of the 28 thermistors in the probe is carried out according to the four vertical sensor sequences. Each sequence comprises seven thermistors, and in the TGI software there is a window where all the calculations can be done for each sequence. Controlling of which registrations are plotted is easily done depending on the functioning of thermistors in the sequence. By one pushbutton

it is possible to remove the average temperature level and the initial time period from the registrations to produce simulation-ready data files.

There are three possible simulation levels in the TGI system. The 1D cylinder symmetric simulation is the quickest and most simple level, whereas 2D simulation is little bit heavier to use. Nevertheless, the results are output in a reasonable time. The third simulation level is a 2D cylinder symmetric configuration, which is the most demanding in terms of model details and computing time. It is possible to decide freely which thermistor results are plotted and applied in modelling. A printing utility makes it possible to print all the results using the MATLAB print commands. Zooming into finer details is possible with respect to each axis separately.

Data interpretations can be run when the analysis part of software is active because all parts of the software are planned to operate independently. Thus, after having started with the “Data analysis” it is possible to freely continue to the interpretation and modelling section of TGI. Interpretations can be done in three levels, 1D cylinder symmetric, 2D and 2D cylinder symmetric case. In the interpretation level all the functions in any open window can be controlled. 1D level is the quickest, however, also the most inaccurate means of modelling due to infinite length of model cylinder. It is often useful to start with the 1D simulations and then continue to 2D models. Further, it is important to keep the number of parameters to be optimised as small as possible in the first calculations and add parameters one by one in the next interpretations. 2D and 2Dc (cylinder case) are more time consuming methods but also more representative of the real probe response. Anisotropy can be included in the models in both 2D models. This, however, is restricted to cylindrical anisotropy where the main components of anisotropy is oriented in the axial and radial directions from the probe.

Further details and instructions of the TGI system can be found in the User's guide (Korpisalo 2005).

4 TEST MEASUREMENTS WITH THE TERO76 LOGGING DEVICE

4.1 Testing of TERO76 in a water-filled tube

The TERO76 probe was tested before drill hole use in a water-filled PVC plastic tube in laboratory. The probe was wrapped in a layer of polyester which is very porous (about 95 %), fibrous and low conductivity material, and placed in a PVC tube (inner diameter 104 mm). The polyester has been observed in earlier studies to prevent convective movement of water during experiments, but it practically does not alter the medium conductivity. For instance, taking a value of 0.3 $Wm^{-1}K^{-1}$ for polyester conductivity, the 95 % water and 5 % polyester mixture has a thermal conductivity of 0.586 instead of the pure water value of 0.607 $Wm^{-1}K^{-1}$ (at 25 ºC).

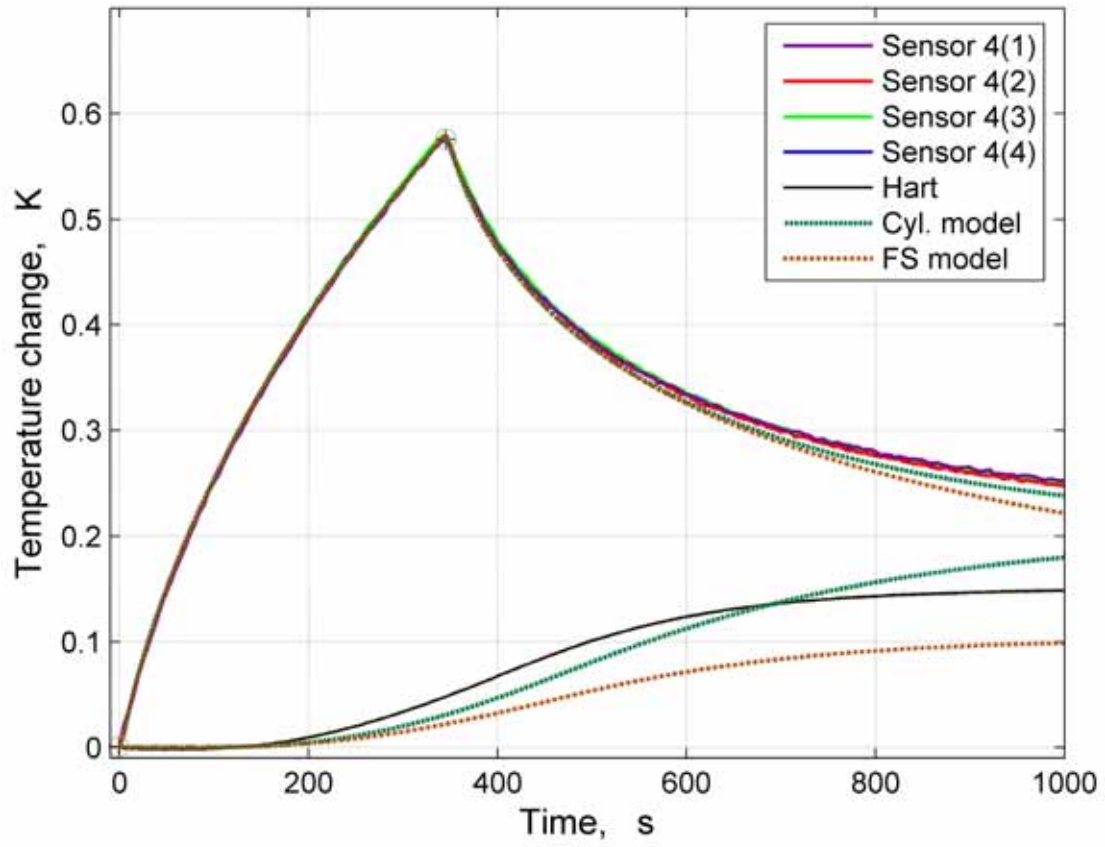

Figure 10. *Response of the TERO76 tool in a water-filled tube (inner diameter 104 mm). The responses of the middle thermistors (Sensor 4(1), 4(2), etc.) are compared with theoretical responses calculated for the tube structure using a cylindrical model (Cyl.) or a homogeneous full space (FS) model with the properties of water at 25ºC, and a reference thermometer reading at the water/PVC contact (Hart). Calculated temperature responses at the reference thermometer location have been included for comparison.*

A short heating experiment was carried out with heating time of 350 s followed by cooling up to 1,000 s. In short times, the probe is expected to react as if it were placed in a full-space with the thermal properties of water. The measured responses show a good agreement with theoretical conductive models calculated for the thermal properties of water during heating time (Figure 10). During cooling the measured probe temperatures are slightly higher, and the difference amounts to about 0.02 K at 1,000 s. The deviation from model results could be attributed to (1) too small heat capacity of the probe in the model, (2) differences between real boundary conditions of the test tube and those assumed in the cylinder model (no flow of heat assumed at outer surface of the PVC tube), or (3) possibly to a small trend in the temperature data. Comparison between the cylindrical model and a homogeneous full space model shows that the full space approximation is valid until about 700 s for probe temperatures. However, temperatures outside the probe differ much earlier, already from about 200 s (Figure 10). Qualitatively, the measured temperatures outside the probe (i.e., at the inner surface of the PVC tube, curve "Hart" in Figure 10), seem to follow better the full space model, although the values do not agree. This could imply that the real boundary condition is not "no-flow" at the PVC tube outer surface but instead there is a heat flow outward. These problems remain to be analysed further in future studies.

We can present here only first results on water-tube testing of the TERO76 tube. Anyhow, the results indicate that the probe works in a reasonable agreement with models and we can proceed to inverting real drill hole measurements.

4.2 Measurements in Olkiluoto, drill hole OL-KR14

Drill hole OL-KR14 was selected as a target for full-scale test measurements with the TERO76 device. The hole has a nominal diameter of 76 mm, a dip of 70º and it intersects mostly migmatitic mica gneiss, granite and tonalite (Niinimäki 2001). The main focus of the in situ measurements was to demonstrate the technical functioning of the new TERO76 probe and to determine the properties of mica gneiss and granitoid rocks at a number of selected depths. A measurement program was designed with an aim to locate homogeneous sections in the drill hole (Table 1).

Seven 1.5 m long sections of the drill hole were chosen for measurements at depths between 394 and 465 m. In this, we used the video images of the drill hole as well as previous single point logs. For repeatability reasons we wanted to have good control of the logging depths and to avoid hydraulically conductive and active fractures possibly disturbing the thermally conductive regime. The sections were selected using the reports on rock types and fractures of the OL-KR14 drill core (Niinimäki 2005) and the flow difference measurements in the hole (Pöllänen and Rouhiainen 2002).

Table 1. *Test measurement program with the TERO 76 probe in drill hole Olkiluoto OL-KR14.*

Drill hole depth/ Date	Rock type[1]	Procedure of measurement	SPR anomaly[2]	Fracturing[3]
394.0 – 395.5 m 26.3.2006	Mica gneiss	Temp. equilibration with probe electronics on, heating 6 h, power 23.2 W.	Minor anomaly at 395 m	No fractures
400.0 – 401.5 m 25.3.2006	Granite (Mica gneiss)	Temp. equilibration with probe electronics on, heating 6 h, power 23.2 W.	No anomaly	No fractures
414.8 - 416.3 m 24.3.2006	Tonalite	Temp. equilibration with probe electronics on, heating 6 h, power 17.5 W.	No anomaly	415.09 – 415.72 m: Two fractures with fillings, one tight fracture
437.5 – 439.0 m 23.3.2006	Tonalite	Temp. equilibration with probe electronics on, heating 6 h, power 21.4 W.	No anomaly	No fractures
439.0 – 440.5 m 27.3.2006	Tonalite	Temp. equilibration with probe electronics on, heating 6 h, power 11.5 W.	No anomaly	No fractures
439.0 – 440.5 m 22.3.2006	Tonalite	Temp. equilibration with probe electronics on, heating 6 h, power 30.6 W.	No anomaly	No fractures
463.1 – 464.6 m 21.3.2006	Granite (Mica gneiss)	Temp. equilibration with probe electronics on, heating 6 h, power 17.6 W.	No anomaly	No fractures

Notes
1) Rock type names according to Niinimäki (2001)
2) Single-point electric resistivity (SPR) log data from Posiva archives.
3) Data from Niinimäki (2001) and Pöllänen and Rouhianen (2002).

The loggings were carried out in March 2006. The TERO76 probe was observed to be functional and it worked well. The friction of the probe packers was found to be considerable, and lowering of the probe in the drill hole was very slow. During measurements, the temperature records were disturbed by high frequency noise ("spikes").

It is unclear whether they were produced by the electronics of the TERO76 device, or by the high voltage power lines in the Olkiluoto area. Such effects were not detected in table testing of the probe. The logging program is summarized in Table 1 and drill hole video images of the measured depths are shown in Figures 11-16.

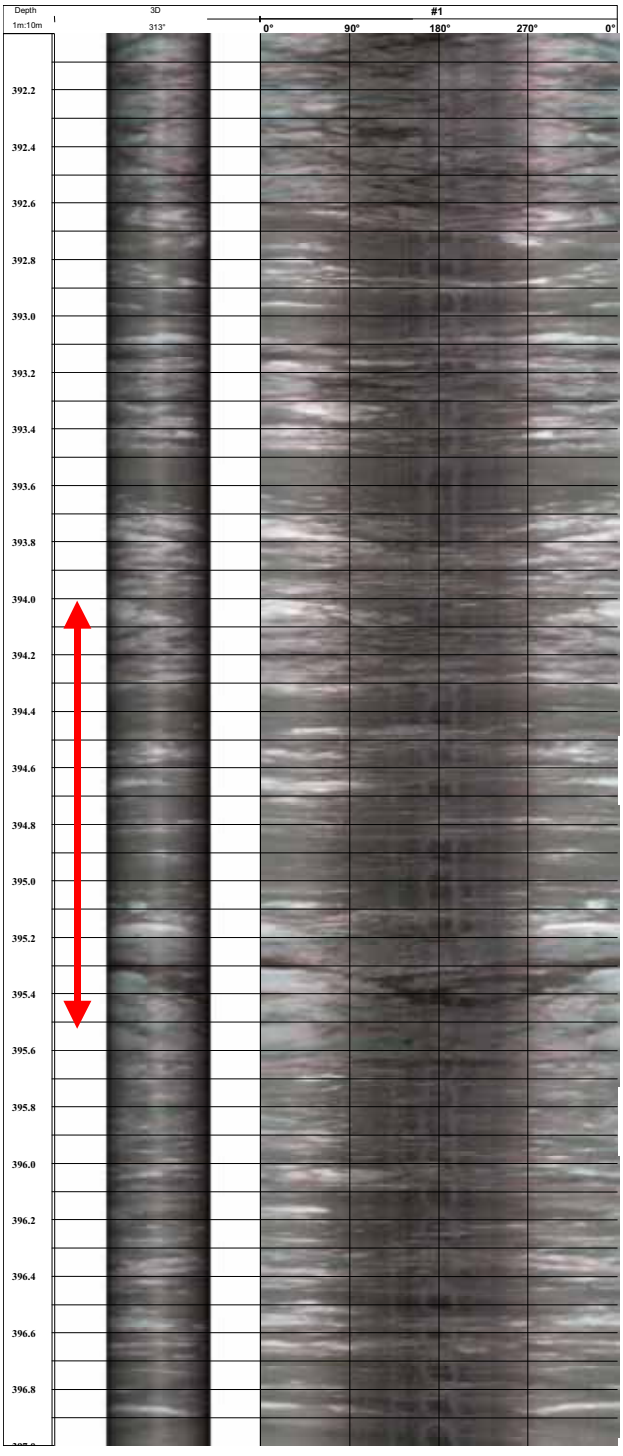

Figure 11. *Drill hole video image of the hole OL-KR14 at the TERO76 measurement depth (mica gneiss) at* 394.0 – 395.5 m (center *394.75 m). The red arrow indicates the measurement interval.*

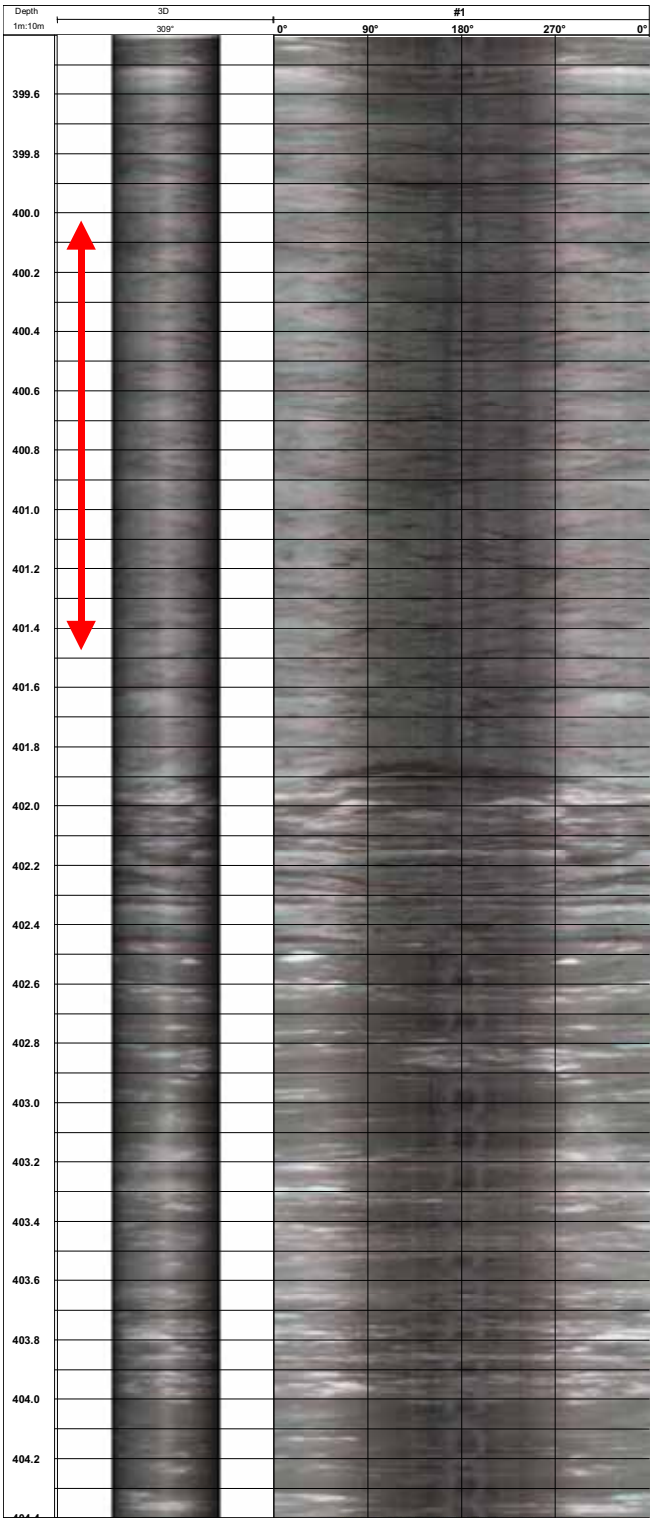

Figure 12. *Drill hole video image of the hole OL-KR14 at the TERO76 measurement depth (mica gneiss/granite) at 400.0 – 401.5 m (center 400.75 m). The red arrow indicates the measurement interval.*

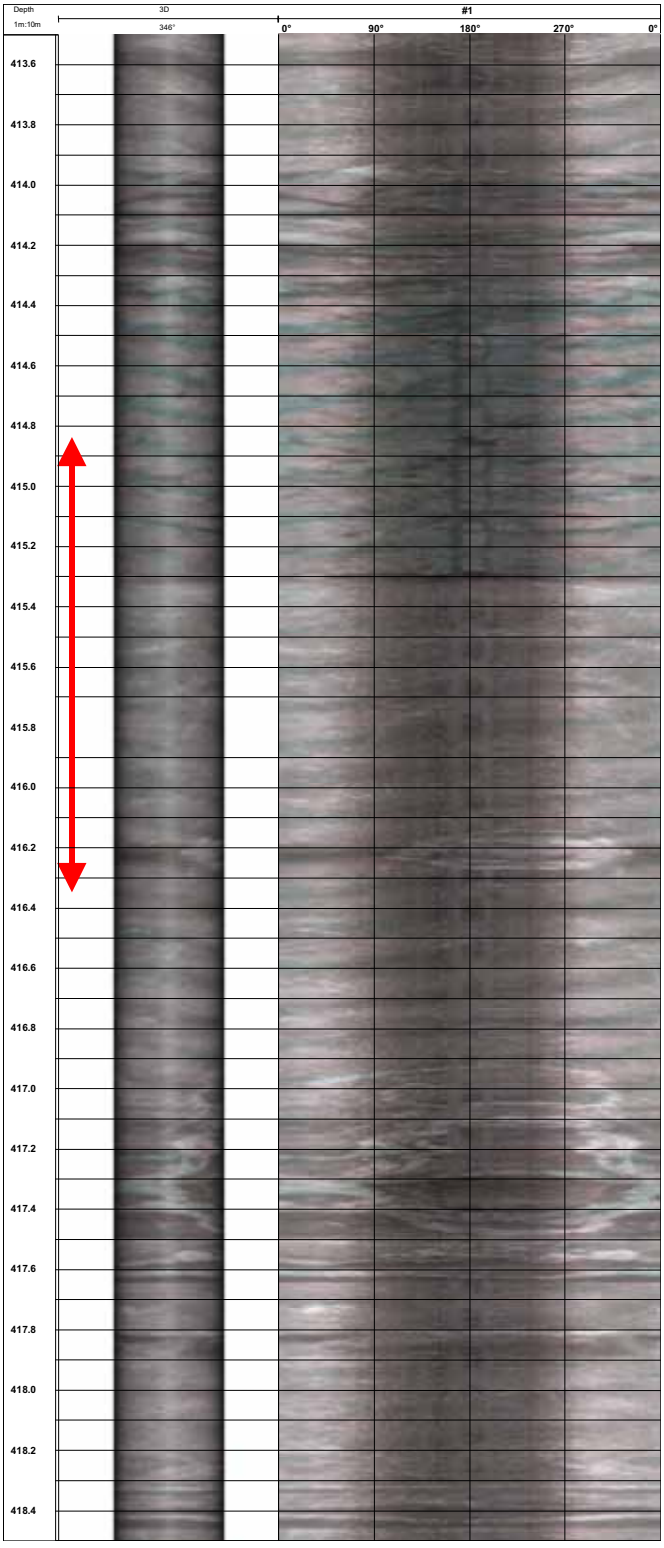

Figure 13. *Drill hole video image of the hole OL-KR14 at the TERO76 measurement depth (tonalite) at 414.8 – 416.3 m (center 415.55 m). The red arrow indicates the measurement interval.*

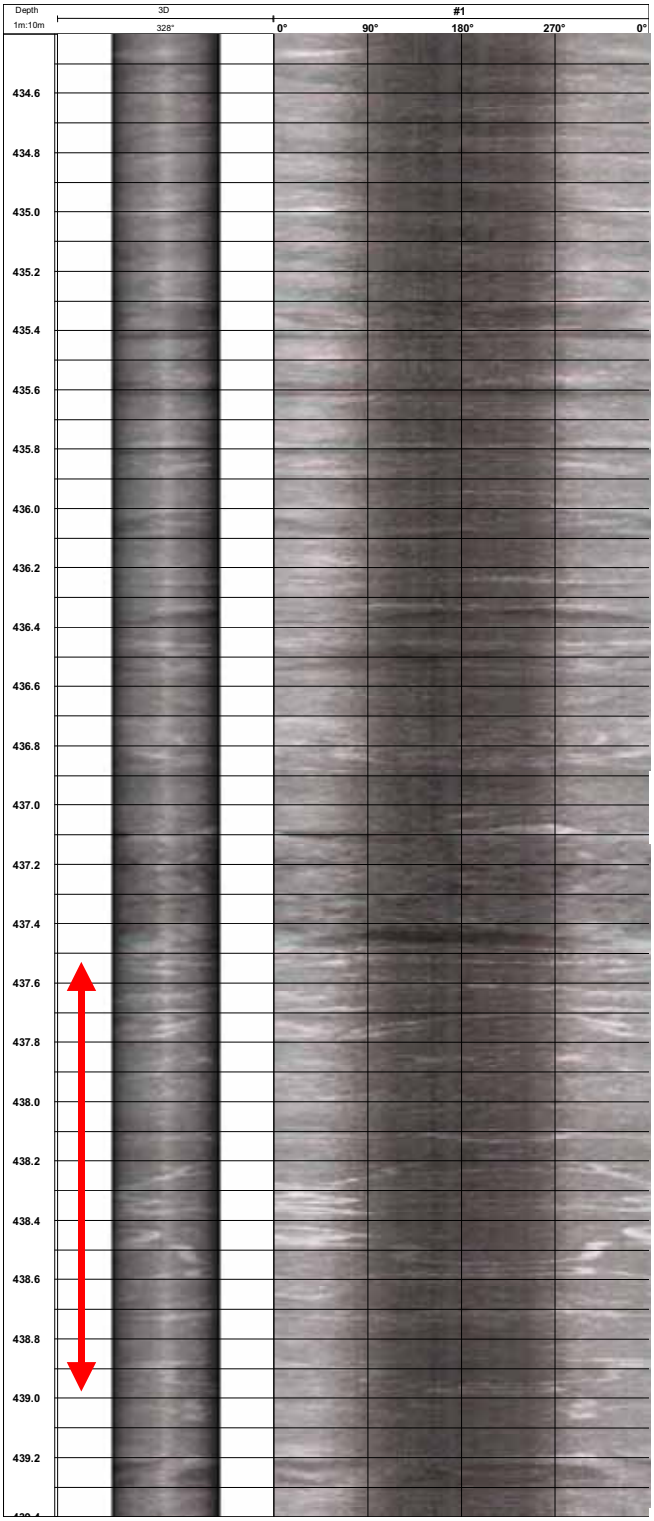

Figure 14. *Drill hole video image of the hole OL-KR14 at the TERO76 measurement depth (tonalite) at 437.5 – 439.0 m (center 438.25 m). The red arrow indicates the measurement interval.*

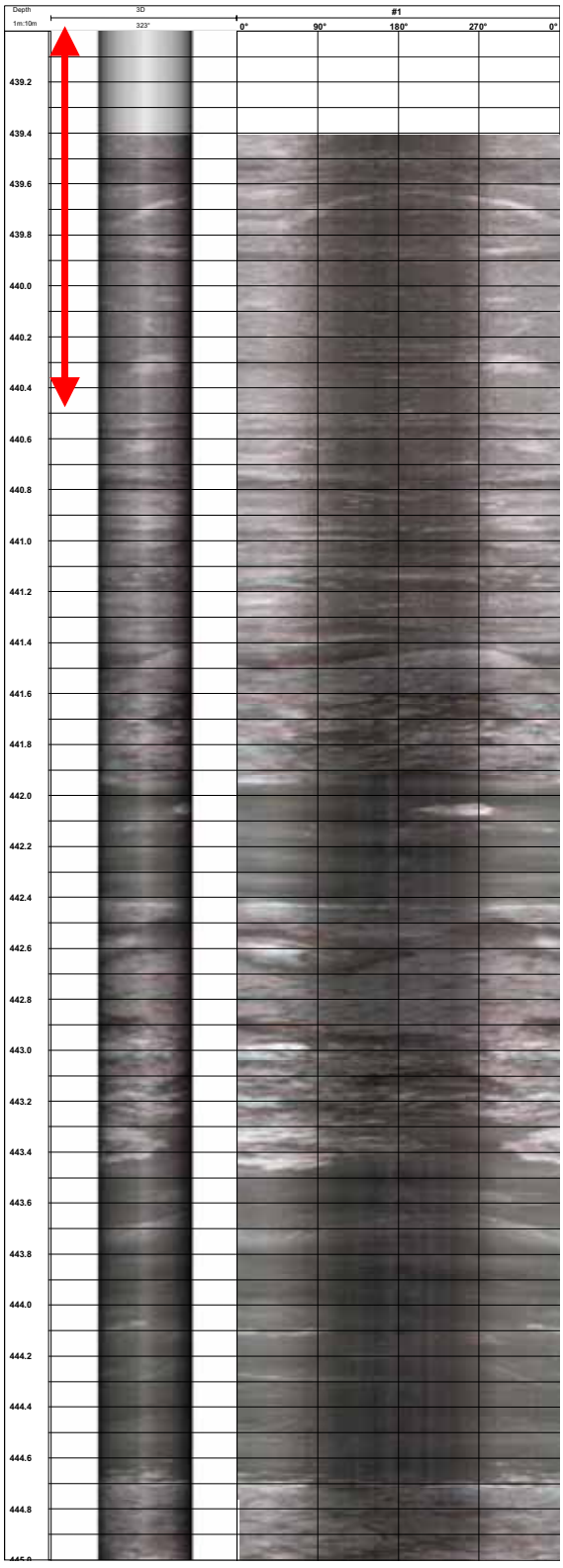

Figure 15. *Drill hole video image of the hole OL-KR14 at the TERO76 measurement depth (tonalite) at 439.0 – 440.5 m (center 439.75 m). The red arrow indicates the measurement interval.*

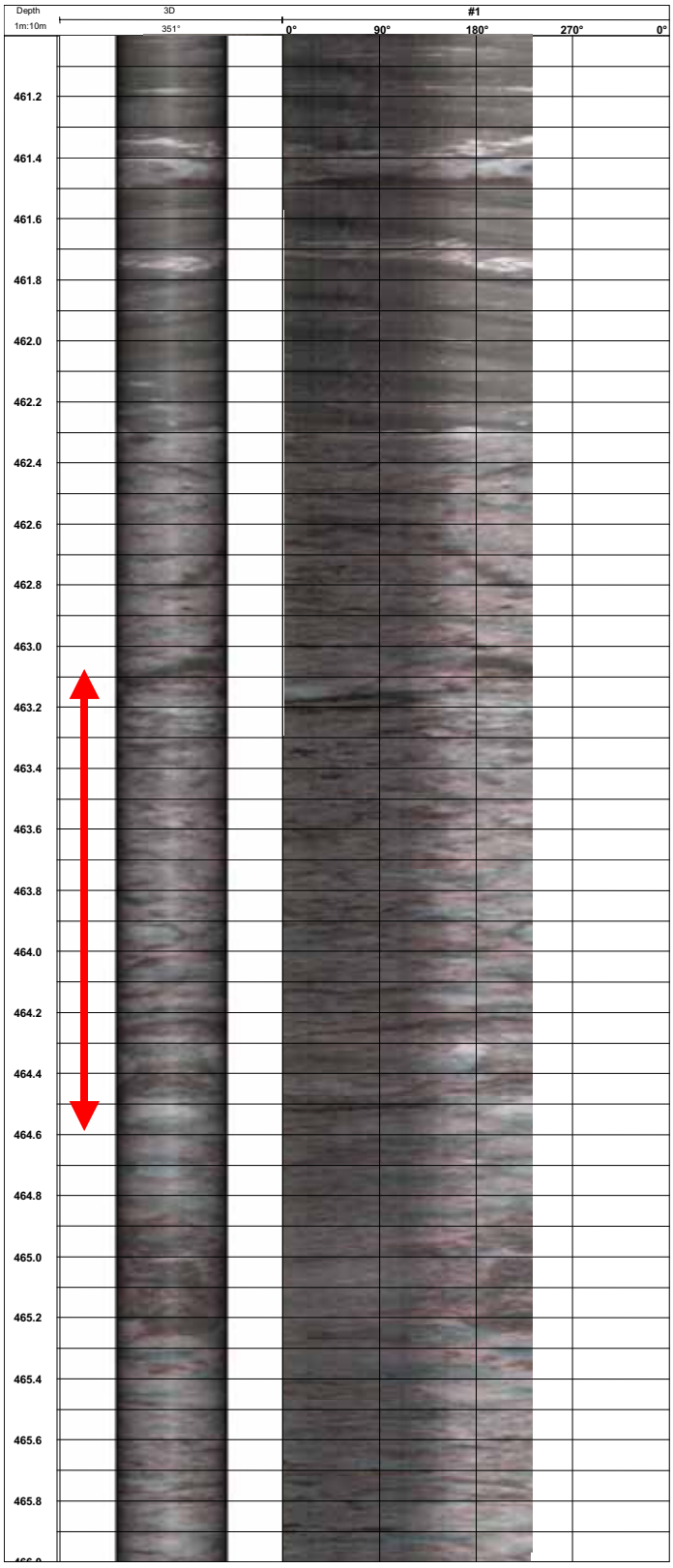

Figure 16. *Drill hole video image of the hole OL-KR14 at the TERO76 measurement depth (granite) at 463.1 – 464.6 (center 463.85 m). The red arrow indicates the measurement interval.*

4.3 Interpretation and discussion of logging results in drill hole OL-KR14

Measurements in OL-KR14 were carried out at six depth levels between 394.0 and 464.6 m (Table 1). The results are shown in Figures 17-30. Deviations from an expected conductive response were detected in five cases. At 394.75 m the thermistors no. 1, 2, 6 and 7 show a sharp change at about 20,000 s (Figure 17). Similar effects are seen at 400.75 m (7,000 s, Figure 19), 438.25 m (19,000 s, Figure 23) and 463.85 m (15,000 s, Figure 29). Such anomalies can be attributed either to a short-term leakage of packers after gradual build-up of pressure and subsequent pulse of water flowing downward, or alternatively, moving of the probe upwards. The effect of such events is qualitatively demonstrated in Figures 31 and 32.

Temporary leakage of packers (fluid flow) produces symmetrical temperature disturbances around the probe centre. Due to the shape of the temperature profile in the probe and in the water column, thermistors in the central part register practically no change in temperature (Figure 31).

On the other hand, if the probe is moved in the drill hole, there will be anomalies looking similar, but they are opposite to the leakage case. When the probe is moved downward, thermistors in the upper part register an increase in temperature, and those in the lower part a decrease, respectively (Figure 32). This is due to changes in temperature differences between the probe and drill hole wall. If the direction of probe movement, or alternatively water flow direction is changed, the anomalies change accordingly.

We can estimate from the recorded temperatures and the vertical temperature profile in the probe and the drill hole wall that the shift of the water column or the probe movement is of the order of a few cm at 394.75, 400.75, 438.25 and 463.85 m (Figures 17-20, 23-24 and 29-30). We prefer here the interpretation that the anomalies are due to minor flow of water between the packers and not to movement of the probe, because the logging data suggest no variations in cable tension or probe depth during the measurements. Moreover, the detected anomalies would require probe movement upward, which we consider unlikely.

The measurements at 415.55 m (Figure 21) show that the temperature ranking of thermistors is not as expected. For instance, the highest temperatures were recorded by the thermistor no. 5, which is not located in the middle of the probe but 24 cm below the middle point. This could be attributed to a continuous slow flow of fluid downward. It is supported by the temperature maps of the probe during both heating and cooling (Figure 22).

The difference flow measurements in the OL-KR14 drill hole (Pöllänen & Rouhiainen 2002) indicate that in the uppermost 50 m there are many hydraulically active fractures and fracture systems from which fluid is flowing into the hole. The flow rates range from 10 to 2000 ml/h. At depths greater than 50 m the flow is directed out from the hole into fractures and the flow rates range from 10 to 2000

ml/h. At the exact depths of our TERO76 measurements no active flow systems were reported in difference flow measurements. The closest active fractures are at 329.6, 448.0, 454.0 and 476.8 m. At these depths the flow rates range from 20 ml/h (329.6 m) to 250-300 ml/h (448.0, 454.0 and 476.8 m) (Pöllänen & Rouhiainen 2002). Assuming that the flow condition in the hole has not changed from the time of the difference flow measurements in 2001, water is probably still flowing out from the borehole into these three fracture systems, which are located beneath the depths of the TERO76 measurements (excluding the deepest one at 463.85 m). With a total flow rate of about 900 ml/h out from the drill hole, a hydraulic head change of about 20 cm/h is expected below the TERO76 measurement depths. How much the water column actually moves depends on the pressure differences between the sections of hole above and below the TERO76 probe as well as the packer retentiveness.

Temperature anomalies showing deviations from simple conductive heat transfer were observed particularly during the heating part of measurements. Such effects were generally not detected in the cooling part, although the thermistor no. 1 shows an abnormal behaviour during cooling at the depth of 438.25 m (Figure 23). It may reflect late leakage effects. The measurements at 439.75 m did not show any non-conductive anomalies (Table 2 and Figures 25-28).

In a perfect conductive situation the thermistors located at symmetric vertical positions around the probe centre would give identical temperature responses. In practice this may be hampered by the leakage and probe movement effects discussed above, but also by instrumental effects. The heating effect of the electronics located at the upper and lower ends of the probe seems to be responsible for the recorded differences between thermistors no. 1 and 7, as well as between thermistors no. 2 and 6. In order to bring the heating effect of electronics to a quasi steady-state situation, the electronics was switched on well before the heating started (Table 1). This may have caused the observed differences in recorded temperature curves (Figures 17-30).

Regardless of the minor disturbances, the measured data could be well used for determination of the rock thermal parameters. The parameter determination is based on fitting measured temperature data with the forward modelling of heat transfer from a heated cylinder with finite length and conductivity (2-dimensional cylinder symmetric finite element model).

The parameter estimation problem is solved as a nonlinear least squares problem. To minimize the misfit between the time dependent measured and modelled temperatures the Levenberg-Marquardt method is applied (e.g. Dennis & Schnabel 1996, Madsen et al. 2004). This damped Gauss-Newton method locally approximates the given nonlinear problem with linear least squares problem. The optimization process iteratively adjusts the unknown model parameters. In every iteration, the first partial derivatives of modelled temperatures with respect to each estimated model parameter are computed. This sensitivity matrix is computed using finite differences. Thus, in every iteration the forward problem is solved N+1 times, where N is the number of unknown parameters. In the present optimisation technique, the strategy is to update

the damping (Marquardt) parameter following the method of Nielsen (1999), otherwise it is based on the algorithm presented by Dennis & Schnabel (1996).

The inverted results are presented in Table 2 and in Figures 17-30. In discussing the inversion results, it should be kept in mind that the fluid flow effects may have produced biasing. In inversions the thermistors located in the middle of the probe (no. 4 in each line of thermistors) were applied. The temperatures of the middle thermistors are least disturbed by possible minor flow and probe movement effects (Figures 31 and 32). The drill hole radius values were kept constant in the inversion using values obtained from drill hole calliper logs at the depths of the TERO76 measurements.

The inverted thermal conductivities range from 2.95 to 3.78 W m^{-1} K^{-1}, and diffusivity from 1.54 to 2.30 $\cdot 10^{-6}$ m^2 s^{-1} (Table 2). The differences between results calculated from the complete heating-cooling cycle and those from the cooling part are small for conductivity (less than 1 %) but higher for diffusivity (up to 13%). In an earlier study, theoretical considerations with simulated data suggested that inversion results from the cooling part are less affected by various sources of bias, such as hole calliper uncertainties (Kukkonen et al. 2005).

At 439.75 m two heating power values were applied (11.5 and 30.6 W, Figures 25-28). The results with the smaller power value yield somewhat smaller conductivities and mostly higher diffusivities than those with the higher heating power value. The differences are smaller than 2 % for conductivity but about 6 % for diffusivity.

Results calculated from temperature sensors on opposite sides of the probe (e.g., 439.75 m, Table 2) are in a good agreement. Differences are much smaller than 1 % for conductivity and smaller than 3% for diffusivity.

The obtained thermal conductivities are in agreement with previous laboratory measurements of rocks in Olkiluoto (Kukkonen & Lindberg 1995, 1998, Kukkonen 2000). The section of OL-KR14 with mica gneiss at 394.75 m shows schistosity more or less perpendicular to the drill hole. Thus, it can be expected that the TERO76 results, which are sensitive particularly for conductivity in the radial direction from the drill hole, would show relatively high value of conductivity in the anisotropic mica gneiss (e.g., Kukkonen & Lindberg 1995, 1998, Kukkonen 2000). This is exactly, what was obtained in the drill hole measurement (3.76 W m^{-1} K^{-1}, Table 2, Fig.17).

Earlier laboratory measurements on thermal conductivity of tonalite and granite (four samples) in Olkiluoto have yielded values in the range of 2.76 – 4.68 W m^{-1} K^{-1} (Kukkonen & Lindberg 1995, 1998). Variations in conductivity can be attributed to variations in contents of quartz and biotite. We can conclude that the present TERO76 results are in general agreement with earlier laboratory measurements of conductivity.

Table 2. *Results of thermal parameter inversions for drill hole OL-KR14.*

Hole depth (m)	Rock type	Thermistor number (line)	Power (W)	t_{Begin} (s)	t_{End} (s)	λ ($Wm^{-1}K^{-1}$)	ρc (Jm^3K^{-1})	s (m^2s^{-1} 10^{-6})	Hrad (mm)	Misfit (K^2)	Notes
394.75	MGN	4(2)	23.2	0	60000	3.78	1796655	2.11	38.0	1.81E-05	1
394.75	MGN	4(2)	23.2	22340	60000	3.76	2068250	1.82	38.0	5.64E-06	1
400.75	GRAN	4(2)	23.2	0	60000	3.70	1744022	2.12	38.0	2.65E-06	2
400.75	GRAN	4(2)	23.2	22340	60000	3.71	1645767	2.25	38.0	5.21E-06	2
415.55	TON	4(2)	17.5	0	60000	3.14	1707312	1.84	38.0	6.71E-06	3
415.55	TON	4(2)	17.5	22340	60000	3.12	1868325	1.67	38.0	1.80E-06	3
438.25	TON	4(2)	21.4	0	60000	3.00	1750769	1.71	38.0	1.40E-06	4
438.25	TON	4(2)	21.4	22340	60000	2.99	1814136	1.65	38.0	1.42E-06	4
438.25	TON	4(4)	21.4	0	60000	2.99	1827138	1.63	38.0	2.01E-06	4
439.75	TON	4(2)	11.5	0	60000	2.95	1724756	1.71	38.0	1.15E-06	
439.75	TON	4(2)	11.5	22340	60000	2.95	1724756	1.71	38.0	1.29E-06	
439.75	TON	4(4)	11.5	0	60000	2.95	1671983	1.76	38.0	2.18E-06	
439.75	TON	4(4)	11.5	22340	60000	2.95	1724756	1.71	38.0	1.05E-06	
439.75	TON	4(2)	30.6	0	60000	3.01	1886037	1.59	38.0	5.64E-06	
439.75	TON	4(2)	30.6	22340	60000	3.00	1951410	1.54	38.0	3.79E-06	
439.75	TON	4(4)	30.6	0	60000	2.99	1981759	1.51	38.0	5.87E-06	
439.75	TON	4(4)	30.6	22340	60000	3.00	1939618	1.55	38.0	2.73E-06	
463.85	GRAN	4(2)	17.6	0	60000	3.52	1533549	2.30	37.9	7.34E-06	5
463.85	GRAN	4(2)	17.6	22340	60000	3.51	1688311	2.08	37.9	2.77E-06	5

MGN is mica gneiss, **GRAN** granite, **TON** tonalite
Sensor indicates the identification number of the sensor (no. of thermistor column in parentheses) used in inversion. Sensors no. 4(2) and 4(4) are on the opposite sides in the middle of the probe.
Power gives the heating power of the probe.
$\mathbf{t}_{\mathbf{Begin}}$ and $\mathbf{t}_{\mathbf{End}}$ indicate which part of heating-cooling cycle was used for inversion.
λ is thermal conductivity, **ρc** volumetric heat capacity, and **s** thermal diffusivity, **Hrad** is drill hole radius value applied in inversion (adapted from OL-KR14 caliper logs), and **Misfit** indicates the degree of fit in inversion
Notes: 1) Packer leakage at 20,000 s, 2) Packer leakage at 7,000 s, 3) Possible packer leakage during the whole experiment, 4) Packer leakage at 19,000 s, 5) Packer leakage at 15,000 s.

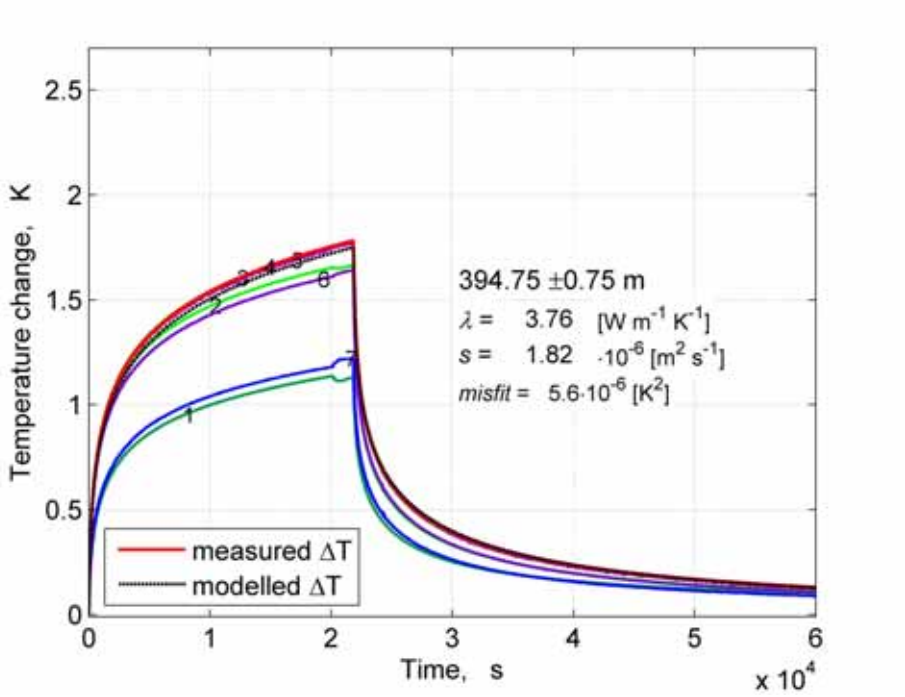

Figure 17*. Measured data from sensor line no. 2 and modelled temperature response of the central thermistor no. 4 during in situ measurement at depth of 394.0 – 395.5 m. The presented conductivity and diffusivity results were inverted from the cooling part. A small packer leakage observed at 20, 000 s.*

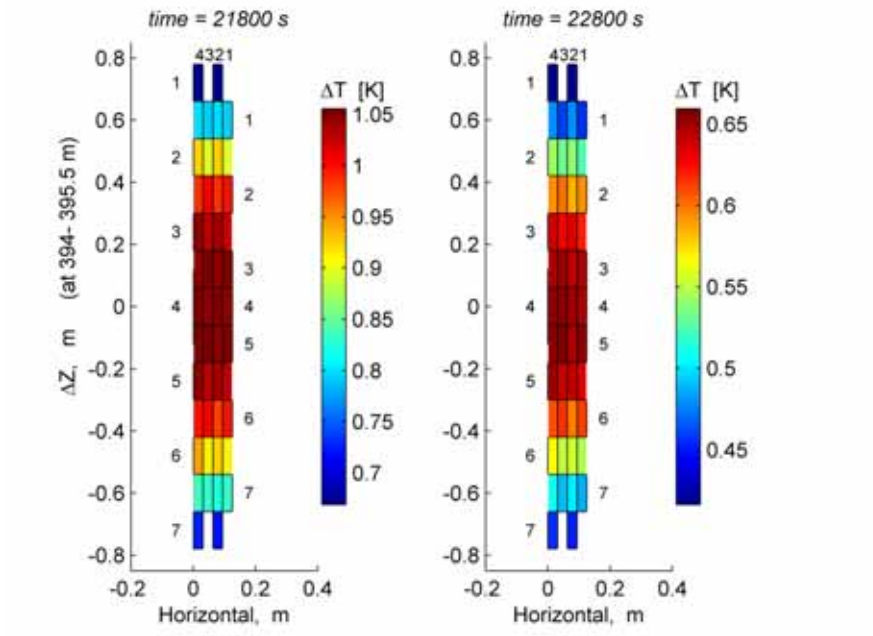

Figure 18. *Maps of temperature changes measured in the probe 100 s before end of heating period (left), and 500 s after beginning of cooling (right). The horizontal numbering (1…4) identifies the vertical lines of thermistors, and vertical numbers, the axial positions, respectively. Depth of measurement 394.0 – 395.5 m.*

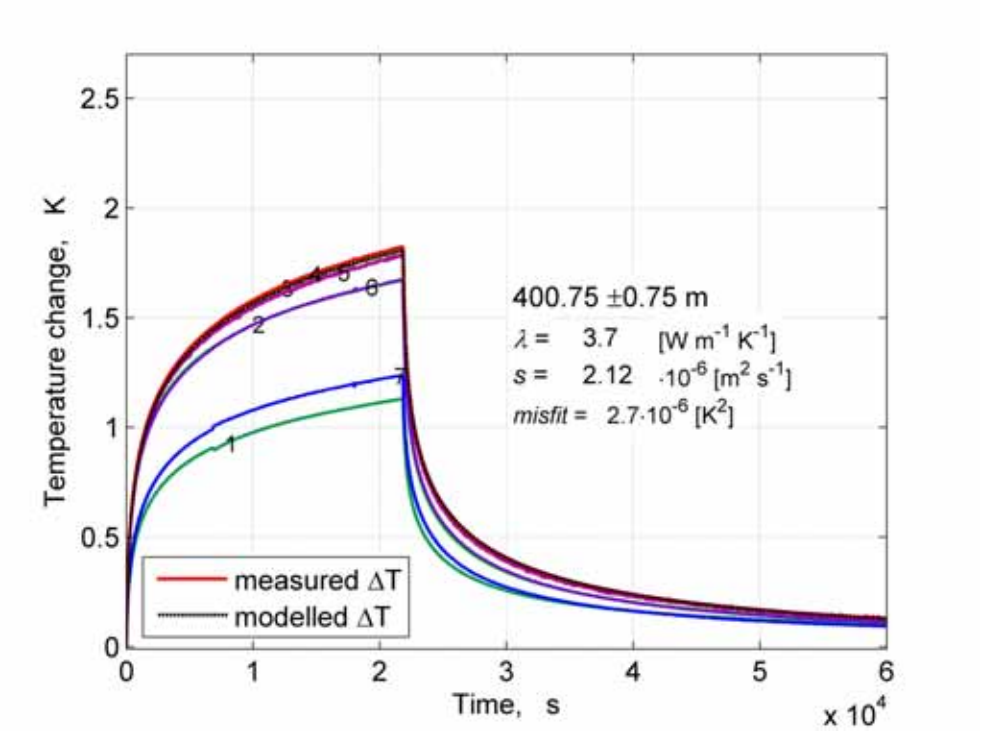

Figure 19. *Measured data from sensor line no. 2 and modeled temperature response of the central thermistor no. 4 during in situ measurement at the depth of 400 – 401.5 m. The presented results were inverted from the cooling part. A small packer leakage observed at 7,000 s.*

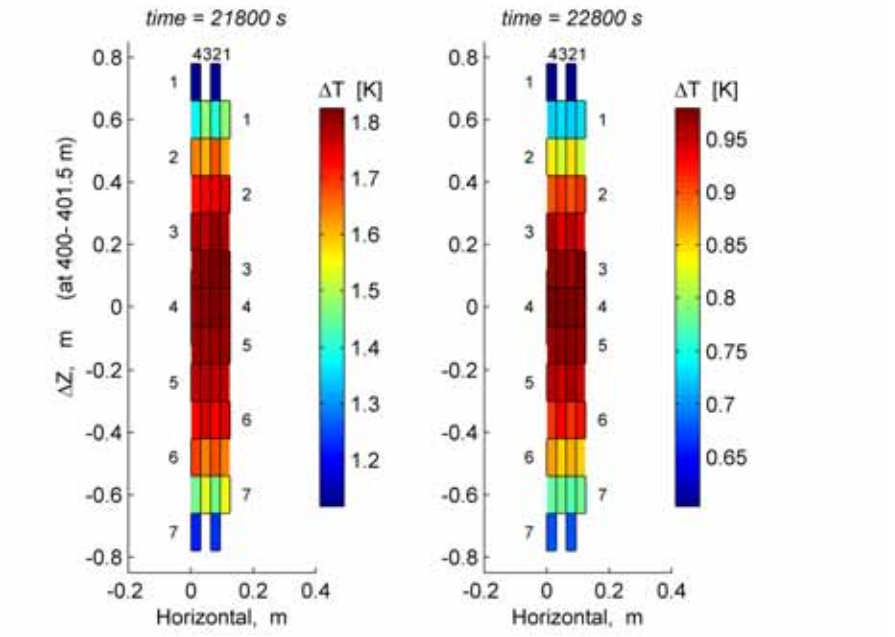

Figure 20. *Maps of temperature changes measured in the probe 100 s before end of heating period (left), and 500 s after beginning of cooling (right). The horizontal numbering (1…4) identifies the vertical lines of thermistors, and vertical numbers, the axial positions, respectively. Depth of measurement 400.0 - 401.5 m.*

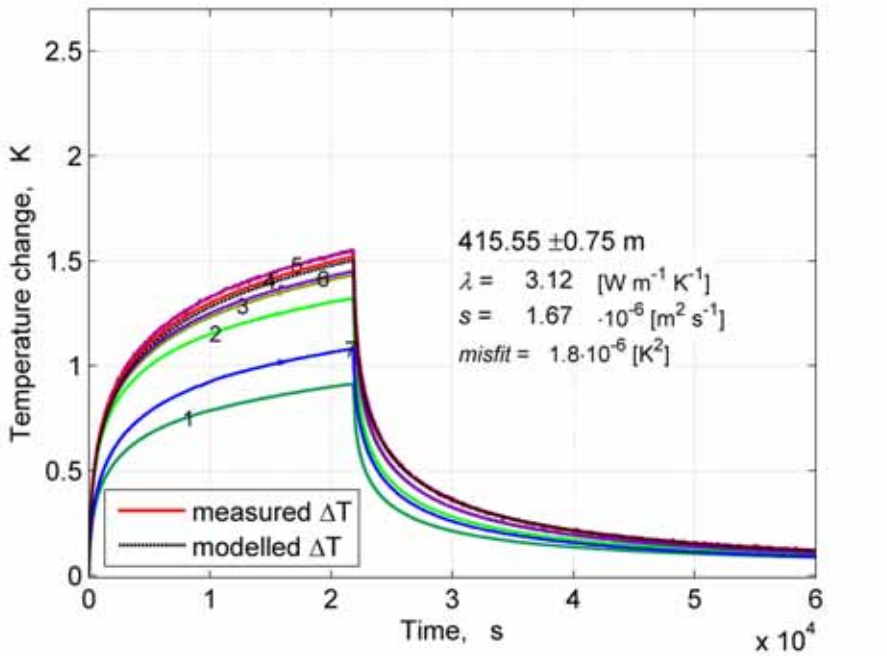

Figure 21. *Measured data from sensor line no. 2 and modeled temperature response of the central thermistor no. 4 during in situ measurement at depth of 414.8 – 416.3 m. The presented results were inverted from the cooling part. The records suggest a constant flow disturbance during the heating experiment (see text).*

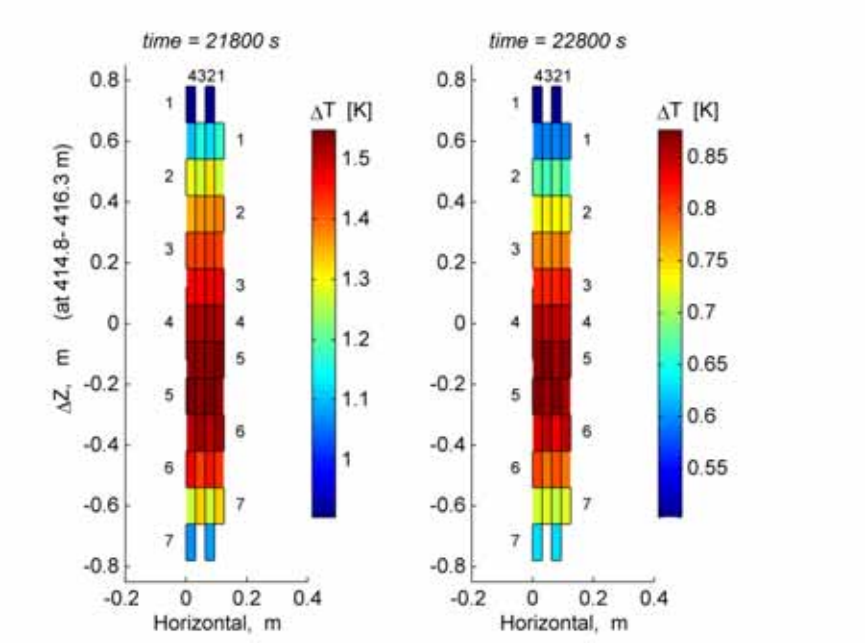

Figure 22. *Maps of temperature changes measured in the probe 100 s before end of heating period (left), and 500 s after beginning of cooling (right). The horizontal numbering (1…4) identifies the vertical lines of thermistors, and vertical numbers, the axial positions, respectively. Depth of measurement 414.8 – 416.3 m.*

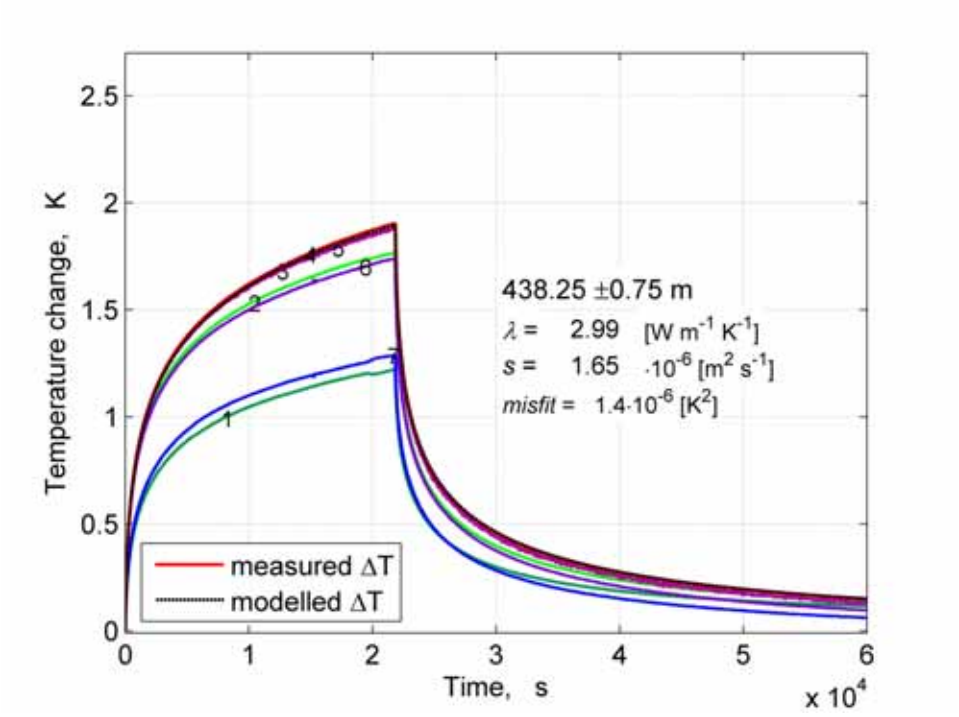

Figure 23. *Measured data from sensor line no. 2 and modeled temperature response of the central thermistor no. 4 during in situ measurement at the depth of 437.5 – 439.0 m. The presented results were inverted from the cooling part. A small packer leakage is observed at 19,000 s.*

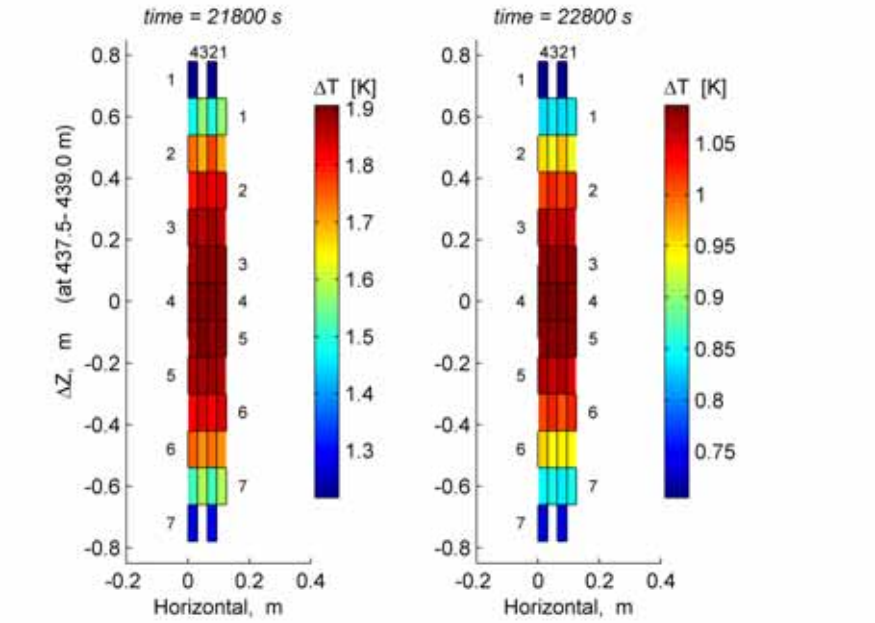

Figure 24. *Maps of temperature changes measured in the probe 100 s before end of heating period (left), and 500 s after beginning of cooling (right). The horizontal numbering (1…4) identifies the vertical lines of thermistors, and vertical numbers, the axial positions, respectively. Depth of measurement 437.5 – 439.0 m.*

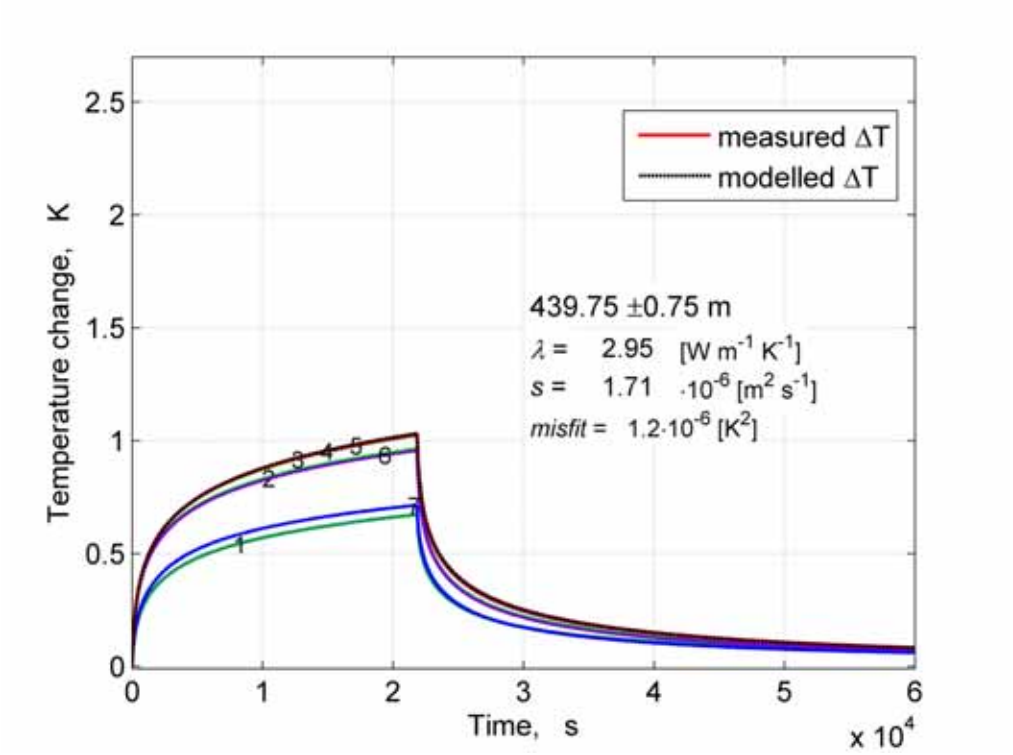

Figure 25*. Measured data from sensor line no. 2 and modeled temperature response of the central thermistor no. 4 during in situ measurement at the depth of 439.0 – 440.5 m. Heating power was 11.5 W. The presented results were inverted from the cooling part.*

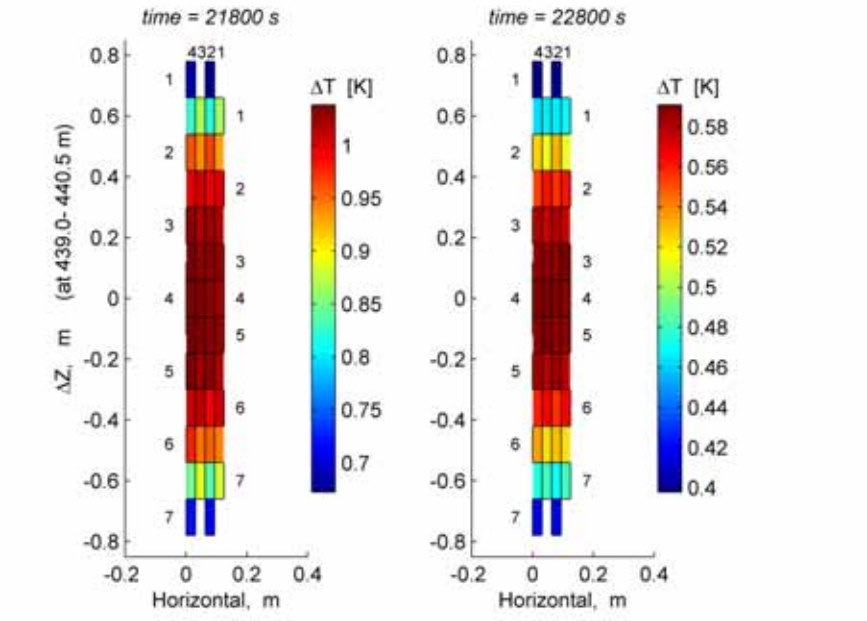

Figure 26. *Maps of temperature changes measured in the probe 100 s before end of heating period (left), and 500 s after beginning of cooling (right). The horizontal numbering (1…4) identifies the vertical lines of thermistors, and vertical numbers, the axial positions, respectively. Heating power was 11.5 W. Depth of measurement 439.0 – 440.5 m.*

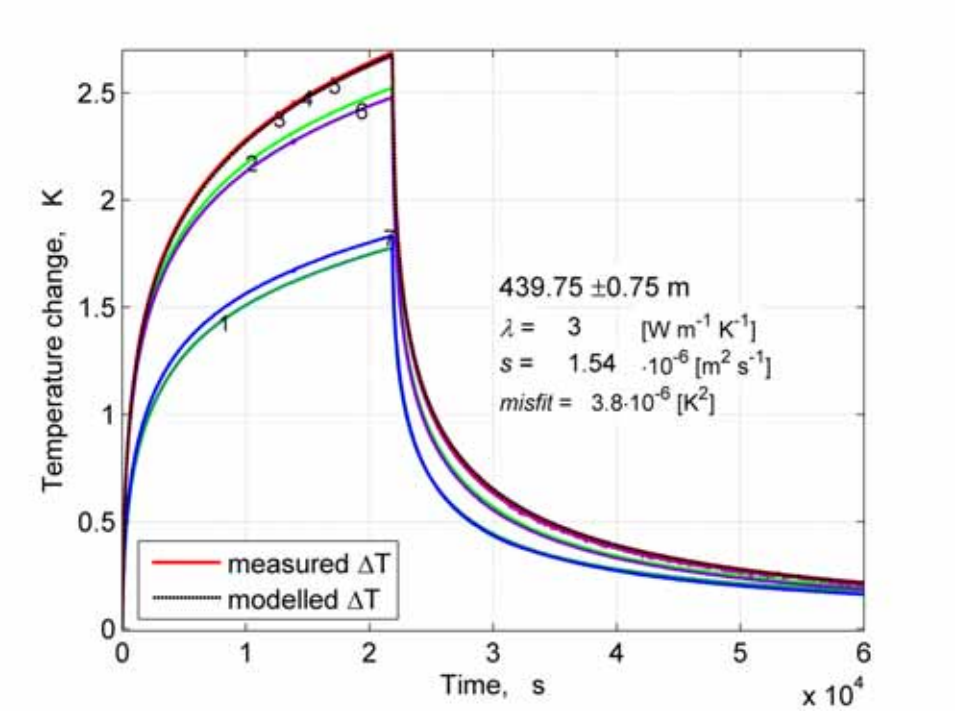

Figure 27*. Measured data from sensor line no. 2 and modeled temperature response of the central thermistor no. 4 during in situ measurement at the depth of 439.0 – 440.5 m. Heating power was 30.6 W. The presented results were inverted from the cooling part.*

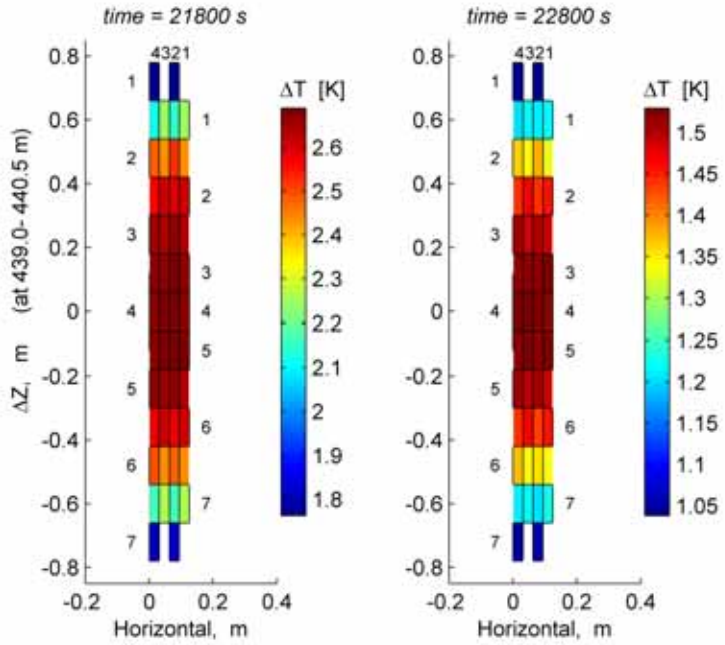

Figure 28. *Maps of temperature changes measured in the probe 100 s before end of heating period (left), and 500 s after beginning of cooling (right). The horizontal numbering (1…4) identifies the vertical lines of thermistors, and vertical numbers, the axial positions, respectively. Heating power was 30.6 W. Depth of measurement 439.0 – 440.5 m.*

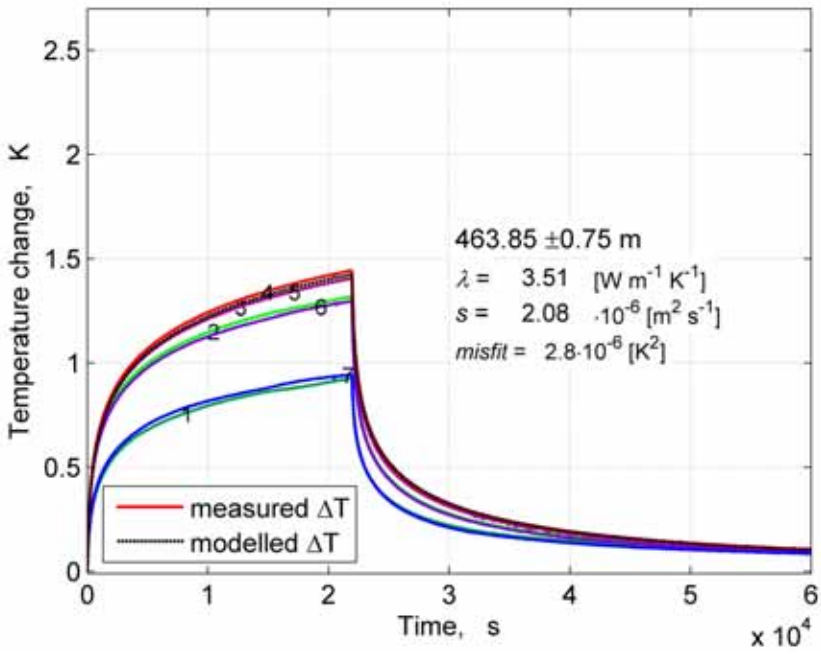

Figure 29. *Measured data from sensor line no. 2 and modeled temperature response of the central thermistor no. 4 during in situ measurement at the depth of 463.1 – 464.6 m. The presented results were inverted from the cooling part. A small packer leakage is observed at 15,000 s.*

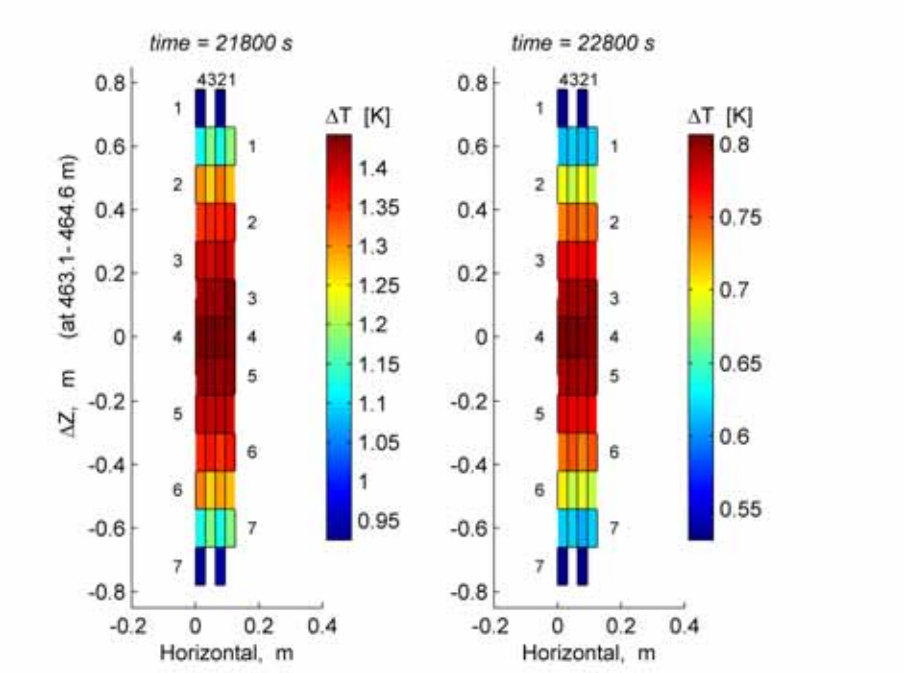

Figure 30. *Maps of temperature changes measured in the probe 100 s before end of heating period (left), and 500 s after beginning of cooling (right). The horizontal numbering (1…4) identifies the vertical lines of thermistors, and vertical numbers, the axial positions, respectively. Depth of measurement 463.1 – 464.6 m.*

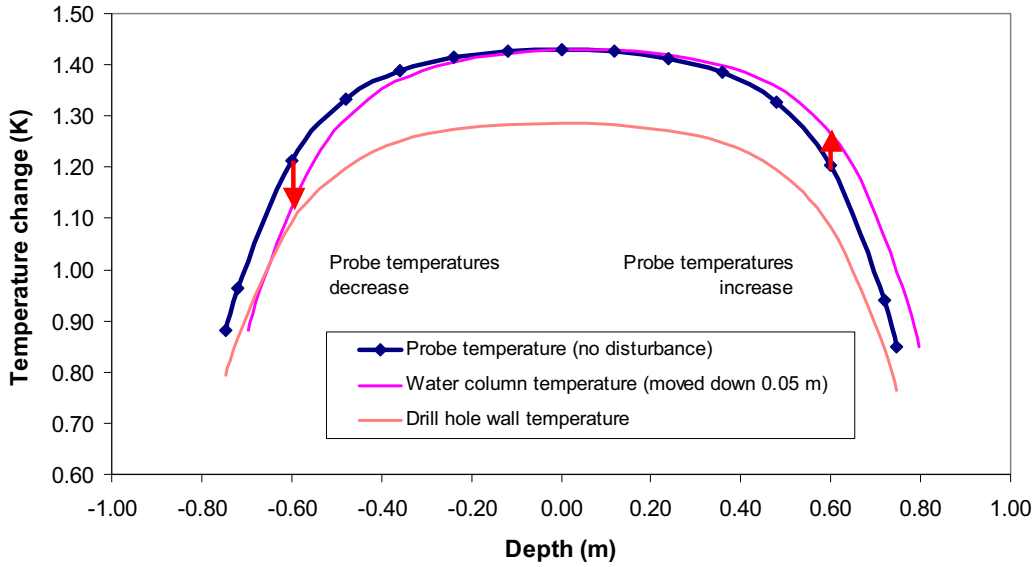

Figure 31. *Qualitative demonstration on how packer leakage affects the recorded temperatures. Probe and drill hole wall temperatures are shown after heating of 18,000 s. Zero depth indicates probe centre. Leakage of packers introduces a shift of the water column (here downward by 5 cm), and the probe temperatures are modified accordingly. In the upper part of the probe, temperatures decrease and in the lower part increase, respectively.*

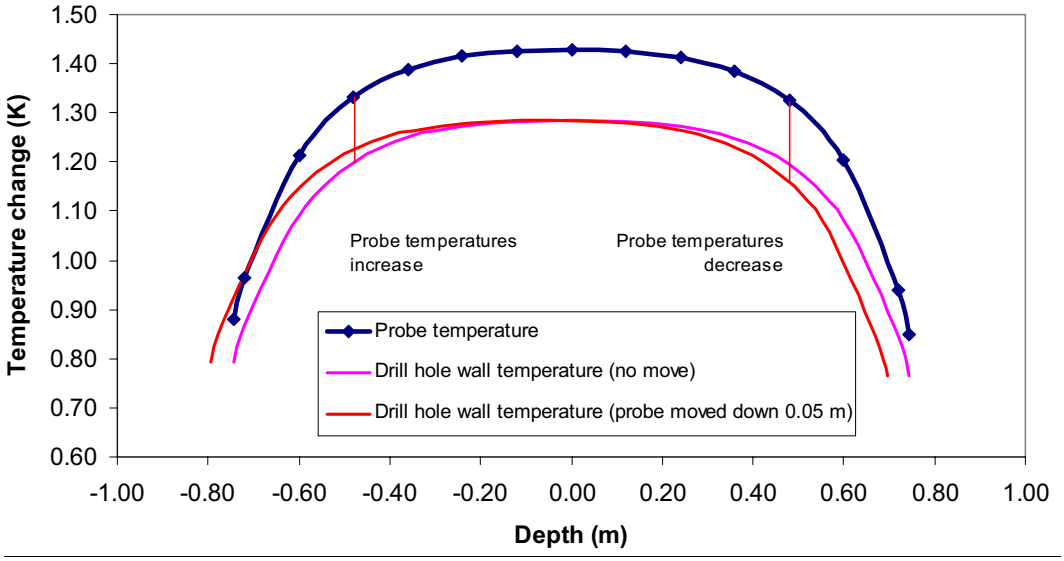

Figure 32. *Qualitative demonstration on how probe movement affects the measurements. Probe and drill hole wall temperatures are shown after heating of 18,000 s. Zero depth indicates probe centre. Movement of the probe (here downward by 5 cm) during heating produces temperature increase in the upper part of the probe and decrease in the lower part, respectively. This is due to the vertical temperature profile of the drill hole wall, which influences the probe temperatures during subsequent heating.*

5 CONCLUSIONS

The present results provide data on mechanical construction, electronics and first drill hole tests of the TERO76 probe. The major differences between the TERO56 and TERO56 probes, in addition to dimensions, are related to the higher maximum heating power, improved measurement technique of the heating power value and the reduced level of undesirable heat generation of the electronics in the TERO76 probe. The device was observed to be technically functional, but a number of problems remain to be improved. For instance, the electronics is still a source of heat disturbing the data records, and in future measurements ways should be sought for reducing the heating effect, for instance by keeping the electronics off during the thermal equilibration before heating.

Leakage of packers may results in disturbed measurements, and special attention should be paid to packer condition and proper functioning. On the other hand, friction of the packers is already considerable in the present construction, and using two pairs of packers does not seem technically possible in inclined drill holes. High friction also creates uncertainty in depth readings. Thus, a compromise must be accepted between packer retentiveness and friction. The mechanical construction and material of the extra weights is also an issue, which needs elaboration. The diameter of the probe centralizers could be made smaller than the present value of 74 mm to reduce the risk of probe getting stuck in typical 76 mm holes. Further, for cases when the probe is stuck in a hole, there should be a special structure in the upper part of the probe, which would break under tensional force lower than the maximum pulling force of the winch and the tensional strength of the cable. Finally, the TERO76 probe, logging cable and winch should to be installed in a trailer for easy transportation and operation.

The first test measurements in drill hole OL-KR14 in Olkiluoto revealed effects of packer leakage in five of the six measurement depths. Alternatively, these temperature anomalies could be attributed to movement of the probe in the hole, but our logging data and available Posiva difference flow measurements support the leakage model. The existing flow systems between the drill hole and bedrock create pressure differences, which occasionally exceed the packer retentiveness and lead to observed anomalies in temperature records. The effects can be considered small, but the inverted thermal property values should be taken with caution. In future development of the TERO56 and TERO76 interpretation, modelling should be elaborated to potentialize also corrections for minor flow effects.

The inverted values of thermal properties are in agreement with previous data on the thermal properties of mica gneiss and granitoid rocks in Olkiluoto. The inverted thermal conductivities range from 2.95 to 3.78 W m^{-1} K^{-1}, and diffusivity from 1.51 to 2.30 $\cdot 10^{-6}$ m^2 s^{-1} .

REFERENCES

Carslaw, H.S. & Jaeger J.C. 1959. Conduction of heat in solids. Oxford University Press, Oxford, 510 p.

Dennis, J. E. & Schnabel, R. B. 1996. Numerical Methods for Unconstrained Optimization and Nonlinear Equations. (Classics in Applied Mathematics 16) SIAM Society for Industrial & Applied Mathematics, Philadephia, 378 p.

Jarny, Y., Ozisik, M.N. & Bardon, J.P. 1991. A general optimisation method using adjoint equation for solving multidimensional inverse heat conduction. Int. J. Heat Mass Transfer 34, 2911-2919.

Kjørholt, H. 1992. Thermal properties of rocks. Teollisuuden Voima Oy, TVO/Site investigations, work report 92-56, 13 p.

Korpisalo, A. 2005. User's Guide: TERO Graphical interface in Matlab/Femlab environment. Geological Survey of Finland, Espoo Office, Geophysical Research, Report Q17/2005/1, 88 p.

Kukkonen, I. 2000. Thermal properties of the Olkiluoto mica gneiss: Results of laboratory measurements. Posiva Oy, Working Report 2000-40, 28 p.

Kukkonen I. & Lindberg A. 1995. Thermal conductivity of rocks at the TVO investigation sites Olkiluoto, Romuvaara and Kivetty. Nuclear Waste Commission of Finnish Power Companies, Report YJT-98-08, 29 p.

Kukkonen, I. & Lindberg, A. 1998. Thermal properties of rocks at the investigation sites: measured and calculated thermal conductivity, specific heat capacity and thermal diffusivity. Posiva Oy, Working Report 98-09e, 29 p.

Kukkonen, I. and Suppala, I. 1999. Measurement of thermal conductivity and diffusivity in situ: Literature survey and theoretical modelling of measurements. Posiva Oy, Report 99-1, 69 p.

Kukkonen I., Suppala I. and Koskinen T. 2001. Measurement of rock thermal properties in situ: numerical models of borehole measurements and development of calibration techniques. Posiva Oy, Working Report 2001-23, 47 p.

Kukkonen, I, Suppala, I., Korpisalo, A. & Koskinen, T. 2005. TERO-vaunu ja TERO76-laitteen tekniset konstruktiopiirustukset. Posiva-työraportti, 2007-xx (in prep.).

Kukkonen, I, Suppala, I., Korpisalo, A. & Koskinen, T. 2006. TERO borehole logging device and test measurements of rock thermal properties in Olkiluoto. Posiva Report, 2005-09, 96 p.

Kukkonen, I., Suppala I., Sulkanen K. & Koskinen T. 2000. Measurement of thermal conductivity and diffusivity in situ: measurements and results obtained with a test instrument. Posiva Oy, Working Report 2000-25, 28 p.

Kukkonen, I., Suppala, I., Korpisalo, A. & Lehtimäki, J. 2006. TERO thermal property measurements in boreholes KAV01 and KLX06 in Oskarshamn. Posiva Oy, Working Report 2006-xx, 26 p. (in press)

Madsen, K., Nielsen, H. B. & Tingleff, O. 2004. Methods for Non-Linear Least Squares Problems, IMM, DTU, 2nd Edition, April 2004. Available at http://www.imm.dtu.dk/courses/02611/nllsq.pdf

Nielsen, H. B. 1999. Damping Parameter in Marquardt's Method. IMM, DTU. Report IMM-REP-1999-05. Available at http://www.imm.dtu.dk/~hbn/publ/TR9905.ps.Z

Niinimäki, R. 2001. Core drilling of deep borehole OL-KR14 at Olkiluoto in Eurajoki 2001. Posiva, Working Report 2001-24, 140 p.

Pöllänen, J. & Rouhiainen, P. 2002. Difference flow and electric condiuctivity measurements at the Olkiluoto site in Eurajoki, boreholes KR13 and KR14. Posiva Working Report 2001-42, 100 p.

Sundberg J., Kukkonen I. & Hälldahl L. 2003. Comparison of thermal properties measured by different methods. Swedish Nuclear Fuel and Waste Management Co, Report SKB R-03-18, 37 p.

Suppala I., Kukkonen I. & Koskinen T. 2004. Kallion termisten ominaisuuksien reikäluotauslaitteisto TERO (Drill hole tool "TERO" for measuring thermal conductivity and diffusivity in situ). Posiva Oy, Working Report 2004-20, 43 p. (in Finnish)